A comparative study of nucleation parameterizations: 1. Examination and evaluation of the formulations

Yang Zhang,[1] Peter H. McMurry,[2] Fangqun Yu,[3] and Mark Z. Jacobson[4]

Received 4 March 2010; revised 20 August 2010; accepted 25 August 2010; published 29 October 2010.

[1] Large uncertainty exists in the nucleation parameterizations that may be propagated into climate change predictions through affecting aerosol direct and indirect effects. These parameterizations are derived either empirically from laboratory/field measurements or from theoretical models for nucleation rates. A total of 12 nucleation parameterizations (7 binary, 3 ternary, and 2 power laws) that are currently used in three-dimensional air quality models are examined comparatively under a variety of atmospheric conditions from polluted surface to very clean mesosphere environments and evaluated using observations from several laboratory experiments and a field campaign conducted in a sulfate-rich urban environment in the southeastern United States (i.e., Atlanta, Georgia). Significant differences (by up to 18 orders of magnitude) are found among the nucleation rates calculated with different parameterizations under the same meteorological and chemical conditions. All parameterizations give nucleation rates that increase with the number concentrations of sulfuric acid but differ in terms of the magnitude of such increases. Differences exist in their dependencies on temperatures, relative humidity, and the mixing ratios of ammonia in terms of both trends and magnitudes. Among the 12 parameterizations tested, the parameterizations of Kuang et al. (2008), Sihto et al. (2006), and Harrington and Kreidenweis (1998) give the best agreement with the observed nucleation rates in most laboratory studies and in Atlanta during a summer season field campaign and either do not exceed or rarely exceed the upper limits of the nucleation rates (i.e., the dimer formation rate) and new particle formation rates (i.e., the formation rate of particles with 2 nm diameter). They are thus the most plausible nucleation parameterizations for applications in the planetary boundary layer of polluted sulfate-rich urban areas. Limitation with the two power laws are that they were derived empirically based on observations at specific locations under certain atmospheric conditions that may be different from laboratory measurement conditions and those at other locations and that they do not consider RH and T dependence. By contrast, the ternary nucleation parameterization of Napari et al. (2002) should not be used because it grossly overpredicts the observed nucleation rates, often exceeding the upper limit dimer or new particle formation rates, and giving an enhancement factor due to the presence of ammonia and a dependence on relative humidity that are inconsistent with laboratory measurements. The binary nucleation parameterization of Wexler et al. (1994) and Kulmala et al. (1998b) also should not be used because the former gives nucleation rates exceeding the upper limits under most atmospheric conditions and the latter contains technical mistakes in its formula.

Citation: Zhang, Y., P. H. McMurry, F. Yu, and M. Z. Jacobson (2010), A comparative study of nucleation parameterizations: 1. Examination and evaluation of the formulations, *J. Geophys. Res.*, *115*, D20212, doi:10.1029/2010JD014150.

1. Introduction

[2] Homogeneous nucleation provides a significant source of new particles and affects number and mass concentrations and size distributions of fine particulate matter ($PM_{2.5}$) that have important chemical, radiative, health, and visibility impacts. Recent studies suggest that nucleation may enhance the concentrations of cloud condensation nuclei (CCN) and cloud droplet number concentrations (CDNC), thus playing an important role in the indirect effect of aerosols on climate

[1]Department of Marine, Earth, and Atmospheric Sciences, North Carolina State University, Raleigh, North Carolina, USA.
[2]Department of Mechanical Engineering, University of Minnesota-Twin Cities, Minneapolis, Minnesota, USA.
[3]Atmospheric Sciences Research Center, State University of New York at Albany, Albany, New York, USA.
[4]Department of Civil and Environmental Engineering, Stanford University, Stanford, California, USA.

0148-0227/10/2010JD014150

[on regional and global scales [e.g., *Laaksonen et al.*, 2005; *McMurry et al.*, 2005; *Spracklen et al.*, 2008; *Yu and Luo*, 2009; *Pierce and Adams*, 2009; *Kuang et al.*, 2009; *Merikanto et al.*, 2009a]. Nucleation can also affect visibility and aerosol direct effect through changing particle size distribution and/or aerosol optical properties such as aerosol optical depth [*Seinfeld and Pandis*, 2006]. The occurrence of nucleation has been widely observed and well documented in a variety of environments such as marine and remote marine boundary layers [e.g., *Raes et al.*, 1997; *Clarke et al.*, 1998; *McMurry et al.*, 2000], coastal areas [e.g., *McGovern*, 1999; *O'Dowd and Hoffmann*, 2005], mountains [e.g., *Weber et al.*, 1997; *Raes et al.*, 1997], boreal forests [e.g., *Mäkelä et al.*, 1997; *Kulmala et al.*, 1998a, 2001a; *Laakso et al.*, 2004; *Sihto et al.*, 2006], free troposphere [*Clarke*, 1992; *Raes et al.*, 1997; *Benson et al.*, 2009], upper troposphere and lower stratosphere [e.g., *Lee et al.*, 2003; *Young et al.*, 2008], remote and moderately polluted continental atmospheres [e.g., *Marti et al.*, 1997; *Birmili and Wiedensohler*, 1998], stack plumes [e.g., *Brock et al.*, 2003], and urban atmospheres [e.g., *McMurry et al.*, 2000; *Weber et al.*, 2003; *Stanier et al.*, 2004; *McMurry and Eisele*, 2005; *Jung et al.*, 2008].

[3] Nucleation mechanisms that have been proposed include binary, ternary, dimer-controlled, cluster-activated, barrierless kinetic, or ion-induced/mediated nucleation. The classical binary nucleation theory is based on the minimization of changes in Gibbs free energy, which is determined by the surface tension of a cluster and saturation ratio of a gas [*Seinfeld and Pandis*, 2006]. This theory has most commonly been applied for the system of sulfuric acid–water vapor (H_2SO_4-H_2O) [e.g., *Jaecker-Voirol and Mirabel*, 1989]. More recently, a kinetic H_2SO_4-H_2O binary homogeneous nucleation (BHN) model constrained by multiple independent laboratory data sets has been developed [*Yu*, 2007]. Growing evidence from field studies has shown that observed nucleation rates often exceed those predicted by classic binary nucleation theory, particularly in the boundary layer [e.g., *Covert et al.*, 1992; *Weber et al.*, 1997; *Clarke et al.*, 1998; *Kulmala et al.*, 1998a; *O'Dowd et al.*, 1999; *McMurry et al.*, 2000]. This has led to speculation that the 3rd species participate in nucleation. The 3rd species may include ammonia (NH_3) [e.g., *Coffman and Hegg*, 1995; *Weber et al.*, 1997, 2003; *Kim et al.*, 1998; *Korhonen et al.*, 1999; *Kulmala et al.*, 2000; *Benson et al.*, 2009], inorganic acids such as hydrochloric acid [e.g., *Arstila et al.*, 1999], organic compounds such as benzoic, *p*-toluic, *m*-toluic acids [e.g., *R. Zhang et al.*, 2004], terpenes [*Marti et al.*, 1997], methane sulfonic acid [e.g., *van Dingenen and Raes*, 1993], iodine-containing compounds [*Hoffmann et al.*, 2001; *O'Dowd et al.*, 2002], and amines [e.g., *Kurtén et al.*, 2008]. Because of the lack of relevant thermodynamic data, predictions of classical ternary nucleation theories contain substantial uncertainties [*Seinfeld and Pandis*, 2006; *Merikanto et al.*, 2007a]. Based on a kinetic ternary nucleation model with NH_3 stabilizing factor constrained by laboratory measurements, *Yu* [2006b] concluded that H_2SO_4–H_2O–NH_3 ternary homogenous nucleation rate is likely to be small in the ambient atmosphere. Dimer-controlled (or "collision-controlled") nucleation theory assumes that stable nuclei are formed when condensable molecules collide. Kinetic theory is used to calculate cluster production rates, and this approach provides an upper limit on nucleation rates [e.g., *McMurry*, 1980, 1983; *Lushnikov and Kulmala*, 1998]. As hypothesized by *Kulmala et al.* [2006], nucleation may occur through the activation of thermodynamically stable clusters via heterogeneous nucleation or heterogeneous chemical reactions including polymerization or activation of soluble clusters, leading to a first-order dependence on H_2SO_4 concentration. Empirically derived dependencies of nucleation rates on H_2SO_4 concentrations from observational data based on cluster-activated [e.g., *Kulmala et al.*, 2006] or barrierless kinetic mechanisms [e.g., *McMurry*, 1980, 1983; *Kuang et al.*, 2008], or both [e.g., *Sihto et al.*, 2006] have been used for atmospheric models, but the key parameters controlling the values of the empirical prefactors (varying by up to 3–4 orders of magnitude based on different measurements) remain to be investigated. Ion-induced or mediated nucleation has also been proposed to explain new particle formation in the troposphere and stratosphere while BHN can also be important in the mid and upper troposphere and lower stratosphere because of lower temperatures. Ion-induced nucleation accounts for enhanced nucleation rates due to Coulombic interactions between small ions and condensing vapors [*Lovejoy et al.*, 2004; *Eisele et al.*, 2006]. Ion-mediated nucleation is based on a kinetic model that explicitly solves the interactions among ions, neutral and charged clusters, vapor molecules, and preexisting particles [e.g., *Yu and Turco*, 2000, 2001; *Yu*, 2006a, 2010]. The role of ion-related nucleation in different environments at different scales remain an open question [e.g., *Eisele et al.*, 2006; *Jung et al.*, 2008; *Yu et al.*, 2008, 2010].

[4] Nucleation parameterizations are derived either empirically from laboratory/field measurements or from the classical/kinetic nucleation models that are based on the aforementioned theories. Use of different nucleation parameterizations in 3-D models give nucleation rates that differ by many orders of magnitude, thus introducing significant uncertainties in the predicted number concentrations of $PM_{2.5}$, particularly in the nuclei mode [*Zhang et al.*, 1999; *Lucas and Akimoto*, 2006; *Elleman and Covert*, 2009a, 2009b; *Yu et al.*, 2010], CCN, and CDNC [*Yu and Luo*, 2009; *Pierce and Adams*, 2009; *Kuang et al.*, 2009]. In this study, seven binary, three ternary, and two power law nucleation parameterizations (one based on kinetic nucleation and one based on cluster-activated nucleation) are first examined under a variety of hypothetical and observed atmospheric/laboratory conditions, then evaluated in a 3-D air quality model, i.e., the U.S. Environmental Protection Agency (EPA) Community Multiscale Air Quality (CMAQ) modeling system, using observations from a sulfate-rich urban environment during summer 1999. The ion-related nucleation parameterization is not included in this study, because the concentrations of large ion clusters observed under such a sulfate-rich urban environment during summer season were too low to act as a significant source of new particles due to high temperatures [*Eisele et al.*, 2006], although ion-related nucleation may be particularly important under conditions with low temperatures and high ion concentrations on a global scale [e.g., *Lee et al.*, 2003; *Yu et al.*, 2010]. In part 1, we describe the nucleation parameterizations, evaluation methodology, and evaluation results under a variety of conditions. Recommendations

are made regarding the appropriateness of the potential applications of these nucleation parameterizations in 3-D models under conditions from very clean to highly polluted environments. Part 2 [*Zhang et al.*, 2010] presents predictions and evaluation of simulated PM volume, number, and surface areas concentrations from the application of 3-D CMAQ with selected nucleation parameterizations for a 1999 summer episode in the southeastern U.S. during which significant nucleation events were observed. Process analysis (PA) is conducted using the PA tool embedded in CMAQ to quantify the contributions of major atmospheric processes that govern the magnitudes and distributions of PM properties. Additional sensitivity simulations are conducted to examine the relative importance of other atmospheric processes such as emissions and dry deposition. Recommendations are also made regarding the appropriateness of these nucleation parameterizations in simulating new particle formation in the real atmosphere representing sulfate-rich polluted environment in the southeastern United States.

2. Nucleation Parameterizations and Evaluation Methodology

[5] It is important to distinguish between nucleation rate and new particle formation rate. The former is the rate at which stable nuclei are formed and cannot currently be measured. The latter is the rate at which detectable particles are formed, and must be smaller than the nucleation rate since some nucleated particles are lost by coagulation with preexisting particles before they can grow to the minimum detectable particle size (~2–4 nm [e.g., *McMurry and Friedlander*, 1979; *Weber et al.*, 1997; *McMurry et al.*, 2000, 2010]). While nucleation could occur on a daily basis, new particle formation occurs only when ambient conditions favor the growth to the minimum detectable size before loss of nucleated particles [*McMurry et al.*, 2010]. The new particle formation rate cannot thus exceed the rate at which molecules collide to form clusters that contain two molecules, i.e., the rate of dimer formation, J_{dimer}, which can be calculated based on the collision-controlled theory of gases [*McMurry*, 1980],

$$J_{\mathrm{dim}er} = \frac{1}{2}\beta_{11}N_1, \tag{1}$$

where β_{11} is the collision frequency function, which is derived from the kinetic theory of gases in the free molecular regime and varies weakly with temperature ($\sim T^{0.5}$), with a typical value of 4.3×10^{-10} cm^3 s^{-1} at 298 K [*McMurry*, 1980], and N_1 is the monomer concentration, in this case, $N_1 = N_{\mathrm{H2SO4}}$, assuming H_2SO_4 is the nucleating species. The value of J_{dimer} provides an upper limit to the rate of new particle formation.

[6] Assuming a minimal detectable size of 2 nm, an upper limit of the new particle formation rate for particles with 2 nm diameter can be estimated based on the collision-controlled theory [see *McMurry*, 1983, Figure 2],

$$J_{2nm} \cong 1 \times 10^{-2} \times R, \tag{2}$$

where R is the monomer formation rate and can be determined as follows:

$$N_1 = 5 \times 10^4 \times R^{1/2}\tilde{N}_1, \tag{3}$$

where N_1 is the monomer concentration of the nucleating vapor (H_2SO_4), $\tilde{N}_1$ is the dimensionless monomer concentration, $\cong 0.44$ based on work by *McMurry* [1980]. Rearranging (3) for R and plugging R into (2) gives

$$\begin{aligned} J_{2nm} \cong 1 \times 10^{-2} \times R &= 1 \times 10^{-2} \times \left(2 \times 10^{-9} \times N_1^2\right) \\ &= 2 \times 10^{-11} \times N_1^2. \end{aligned} \tag{4}$$

[7] Note that both J_{dimer} and $J_{2\ \mathrm{nm}}$ depend strongly on N_1. They either do not depend or insignificantly depend on temperature, relative humidity, and pressure. The nucleation rates could exceed J_{dimer} if species other than H_2SO_4 were to dominate the nucleation process. It is possible that this may occur in regions such as coastal areas where iodine-containing species might dominate nucleation. This is because iodine oxide (I_2O_4), produced from the photodissociation of CH_2I_2 in coastal atmosphere, can nucleate and readily condense to rapidly grow particles [*Hoffmann et al.*, 2001]. Similarly, HI and HOI can readily condense and remain in the condensed phase [*McFiggans et al.*, 2000]. However, it is unlikely that such nucleation processes overall play a major role in the continental boundary layer. The values of new particle formation rates from various nucleation parameterizations should be smaller than J_{dimer} and either smaller than or equal to $J_{2\ \mathrm{nm}}$, they are otherwise unrealistic. Most current 3-D air quality models do not account for nucleated particle loss by collision as they grow to the minimal detectable particle size, so the particle number concentrations simulated by the nucleation parameterizations depend on the minimal detectable particle size assumed in these models. As an example, CMAQ assumes a minimal detectable particle diameter of 2 nm to calculate the new particle formation rates using work by *Kulmala et al.* [1998b].

[8] The seven BHN parameterizations examined in this study included those of *Wexler et al.* [1994], *Pandis et al.* [1994], *Fitzgerald et al.* [1998], *Harrington and Kreidenweis* [1998], *Kulmala et al.* [1998b], *Vehkamäki et al.* [2002], and *Yu* [2008] (referred to as WE94, PA94, FI98, HK98, KU98, VE02, and YU08, respectively). The three ternary homogeneous nucleation (THN) parameterizations include those of *Napari et al.* [2002], *Merikanto et al.* [2007b], and *Yu* [2006b] (referred to as NA02, ME07, and YU06, respectively). The two observation-based power law parameterizations include those of *Sihto et al.* [2006] and *Kuang et al.* [2008] (referred to as SI06 and KU08, respectively). Table 1 summarizes the theoretical bases and formulation features of these parameterizations along with their host 3-D air quality models. All these parameterizations have been used to calculate J for particles in 3-D air quality models (see Table 1 and references therein). Some parameterizations indicate explicitly that J is for particles with diameter of 1 nm (i.e., $J_{1\ \mathrm{nm}}$) and some do not specify the particle size but using the term of nucleation rates. The early growth of particles from 1 nm to the

Table 1. Binary, Ternary, and Power Law Nucleation Parameterizations for 3-D Air Quality Models[a]

Type	Parameterization	Formulation and Theoretical Basis	3-D Host Model/Reference
Binary	*Wexler et al.* [1994] (WE94)	$J = (C_{sulf} - C_{sulf,\ crit}) \times C_{unit} \times \Delta t$, where $C_{sulf,crit} = \exp(\chi)$, $\chi \propto f(T, RH)$, first-order polynomial of T and RH based on work by *Jaecker-Voirol and Mirabel* [1989]; nucleation only occurs when $C_{sulf} > C_{sulf,\ crit}$,	CIT [*Griffin et al.*, 2002]
	Pandis et al. [1994] (PA94)	$\log_{10}$, $J \propto f(RH, N_{H2SO4})$, first-order polynomial of RH and $\log_{10}$ (N_{H2SO4}); no T dependence; based on work by *Jaecker-Voirol and Mirabel* [1989]	GATOR; NCSU adaptations of CMAQ-v4.4, v4.7 [*Jacobson*, 1997, 2001, 2004]
	Fitzgerald et al. [1998] (FI98)	$\log_{10}$, $J \propto f(N_{H2SO4}, T, RH)$, a polynomial with first-order of $\log_{10}$ (N_{H2SO4}), and second-order polynomial of log (RH) and T; based on work by *Jaecker-Voirol and Mirabel* [1989]	GATOR; NCSU adaptations of CMAQ-v4.4, and v4.7 [*Jacobson*, 1997, 2001, 2004; *Zhang et al.*, 2009, 2010]
	Harrington and Kreidenweis [1998] (HK98)	$\Delta N_1^N = J_{crit}\ \Delta t_n$ where $J_{crit} \propto f(C_{sulf,crit}, T, RH)$, based on work by *Jaecker-Voirol and Mirabel* [1989] and $\Delta t_n \propto f(V_{crit}, J_{crit}, T, RH)$, $C_{sulf,\ crit}$ and Δt_n are obtained by solving for a coupled gas-PM system for 2 PM modes with 2 moments (number/mass) and condensational growth	U.S. EPA CMAQ v4.3 and older; NCSU adaptations of CMAQ-v4.4 and v4.7 [*Binkowski and Roselle*, 2003; *Byun and Schere*, 2006; *Zhang et al.*, 2009, 2010]
	Kulmala et al. [1998b] (KU98)	$J = \exp(\chi)$, where $\chi \propto f(N_{H2SO4}, T, RH, X_{crit})$, first-order polynomial of ln (N_{H2SO4}), T, RH, and X_{crit}, based on a classical binary homogeneous nucleation model	U.S. EPA CMAQ, v4.4–v4.7 [*Binkowski and Roselle*, 2003; *Byun and Schere*, 2006]
	Vehkamäki et al. [2002] (VE02)	$J = \exp(\chi)$, where $\chi \propto f(N_{H2SO4}, T, RH, X_{crit})$, a polynomial with first-order of ln (N_{H2SO4}) and X_{crit}, and third-order of ln (RH), ln (N_{H2SO4}), and T, based on classical binary homogeneous nucleation model	GATOR-GCMOM; NCSU adaptations of CMAQ-v4.4 and v4.7; CMU GISS GCM II-prime with TOMAS [*Jacobson*, 1997, 2001, 2004; *Zhang et al.*, 2009, 2010; *Pierce and Adams*, 2009]
	Yu [2008] (YU08)	$J \propto f(N_{H2SO4}, T, RH)$, Lookup table of J values based on an analytical representation of quasi-unary homogeneous nucleation rates constrained with laboratory measurements	NCSU adaptations of CMAQ-v4.4 and v4.7; GEOS-Chem [*Zhang et al.*, 2009, 2010; *Yu and Luo*, 2009; *Yu et al.*, 2010]
Ternary	*Napari et al.* [2002] (NA02)	ln $J \propto f(N_{H2SO4}, C_{NH_3}, T, RH)$, a polynomial with third-order of T, second-order of ln (N_{H2SO4}), ln (C_{NH3}), and first-order of RH and ln (RH); based on a classical ternary homogeneous nucleation model	NCSU and UW adaptations of CMAQ-v4.4; GATOR-GCMOM; CMU GISS GCM II-prime with TOMAS [*Zhang et al.*, 2009, 2010; *Elleman and Covert*, 2009a, 2009b; *Jacobson*, 1997, 2001, 2004; *Pierce and Adams*, 2009]
	Merikanto et al. [2007b] (ME07) with corrections by *Merikanto et al.* [2009b]	ln $J \propto f(N_{H2SO4}, C_{NH_3}, T, RH)$, a polynomial with third-order of T and ln (C_{NH3}); second-order of ln (N_{H2SO4}); first-order of RH, ln (RH); updated parameterization of NA02 based on a classical ternary homogeneous nucleation model. Note that "RH" is missing from the term involving $f_{15}(T)/\xi^3 \ln c$ in equation (8) in ME07, which should be corrected to be "$f_{15}(T)\ RH/\xi^3 \ln c$")	NCSU adaptations of CMAQ v4.4 and v4.7; UW adaptation of CMAQ v4.4 [*Zhang et al.*, 2009, 2010; *Elleman and Covert*, 2009a, 2009b]
	Yu [2006b] (YU06)	$J \propto f(N_{sulf}, T, RH)$, Lookup table of J values based on a kinetic ternary homogeneous nucleation model with the NH_3 stabilization effect ($F_{NH3} = 2$) constrained with laboratory measurements	NCSU adaptations of CMAQ v4.4 and v4.7 [*Zhang et al.*, 2009, 2010]
Power Law (activation or kinetic)	*Sihto et al.* [2006] (SI06)	$J \propto A \times (N_{sulf})$, first-order for N_{sulf}, assuming activation type nucleation, i.e., activation of small clusters via heterogeneous nucleation or chemical reactions, where $A = 1.7 \times 10^{-6}$	NCSU adaptations of CMAQ v4.4 and v4.7 and GU-WRF/Chem [*Y. Zhang et al.*, 2004, 2009, 2010]
	Kuang et al. [2008] (KU08)	$J \propto K \times (N_{sulf})^{2.01}$, second-order for N_{sulf}, assuming kinetic type nucleation, i.e., critical clusters are formed by collisions of H_2SO_4 or other molecules containing H_2SO_4, e.g., NH_4HSO_4, where $K = 1.6 \times 10^{-14}$	NCSU adaptations of CMAQ v4.4 and v4.7 [*Zhang et al.*, 2009, 2010]

[a] J, new particle formation rate, $cm^{-3}\ s^{-1}$; C_{sulf}, the concentration of H_2SO_4 in $\mu g\ m^{-3}$, $C_{sulf,crit}$, the critical concentration of H_2SO_4 in $\mu g\ m^{-3}$ needed to produce $J = 1\ cm^{-3}\ s^{-1}$; C_{unit}, the unit conversion factor; Δt – time step for nucleation calculation in s; N_{H2SO4}, H_2SO_4 number concentration, cm^{-3}; X_{crit}, the H_2SO_4 mole fraction in the critical nucleus; J_{crit}, the critical nucleation rate in particles $cm^{-3}\ s^{-1}$; Δt_n, the length of the nucleation event; ΔN_1^N, the total number of particles formed during time period of Δt_n; C_{NH3} or ξ, NH_3 volume mixing ratio, ppt; $N_{cluster}$, molecular cluster concentrations; T, temperature, °C; RH, relative humidity, % or as fraction; CIT, the California/Carnegie-Mellon Institute of Technology Air Quality Model; CMAQ, Community Multiscale Air Quality Modeling System; GATOR-GCMOM, the Gas, Aerosol, TranspOrt, Radiation, General Circulation, Mesoscale, and Ocean Model; GU-WRF/Chem-MADRID, the Global-through-Urban Weather Research and Forecasting model with Chemistry with the Model of Aerosol Dynamics, Reaction, Ionization and Dissolution; GISS GCM II-prime with TOMAS, the Goddard Institute for Space Studies II-prime General Circulation Model the TwO-Moment Aerosol Sectional microphysics model; EPA, the U.S. Environmental Protection Agency; NCSU, North Carolina State University; CMU, Carnegie Mellon University; and UW, University of Washington.

detectable size ranges of 2–4 nm is not explicitly simulated in most models, which either assume a minimal size of 2 nm or larger or directly place new particles in the smallest size range simulated in the model to produce new particles.

[9] The BHN parameterizations of WE94, PA94, FI98, and HK98 are based on the same set of calculations of J performed by *Jaecker-Voirol and Mirabel* [1989], which calculates the absolute nucleation rates based on heteromolecular homogeneous nucleation theory of the H_2SO_4–H_2O system. Therefore, differences in the nucleation rates from these parameterizations originate from the algorithms used to parameterize them. For example, PA94 does not account for the dependence of J on temperature, T, which is considered in other parameterizations but with different mathematical expressions. KU98 is the default nucleation parameterization used in CMAQ version 4.3 and newer. It is valid for J of 10^{-5}–10^{5} cm^{-3} s^{-1} under the atmospheric conditions with T of 233.15–298.15 K and relative humidity (RH) of 10–100%. KU98 and VE02 are derived based on the classical BHN model that simulates nucleation kinetics and accounts for hydration. In addition to several approximations, the derivation of KU98, however, contained a mistake in the kinetic treatment for hydrate formation (i.e., the terms corresponding to free H_2SO_4 and water molecules were missing in the diagonal terms of the growth tensors that account for collision between free H_2SO_4 molecules and between water molecules), leading to 1–3 orders of magnitude too low nucleation rates [*Vehkamäki et al.*, 2002; *Noppel et al.*, 2002]. This mistake was corrected by VE02, which is valid for J of 10^{-7}–10^{10} cm^{-3} s^{-1} under the atmospheric conditions with T of 230.15–305.15 K, RH of 0.01–100%, and the number concentration of H_2SO_4 (N_{H2SO4}) of 10^{4}–10^{11} cm^{-3}. The temperature has been extrapolated down to 190 K for its application in upper troposphere and stratosphere [*Vehkamäki et al.*, 2002]. FI98 is most accurate in the range of 273–303 K and 60–100% RH [*Fitzgerald et al.*, 1998]. YU08 assumes that H_2O concentrations are sufficiently high that BHN can be treated as a quasi-unary nucleation (QUN) process for H_2SO_4 in equilibrium with H_2O and calculates J based on an analytical representation of QUN rates with key thermodynamic parameters constrained by multiple laboratory measurements. The lookup table of YU08 covers J values under atmospheric conditions with N_{H2SO4} of 10^{5}–10^{9} cm^{-3} for T of 190–310 K and N_{H2SO4} of 10^{9}–10^{12} cm^{-3} for T of 280–310 K, both with RH of 1–99% [*Yu*, 2008]. Different from other BHN parameterizations, HK98 accounts for condensational growth of the particles in calculating the critical nucleation rate and the length of the nucleation event.

[10] The THN parameterization of NA02 is valid for atmospheric conditions with T of 240–300 K, RH of 0.05–0.95, N_{H2SO4} of 10^{4}–10^{9} molecules cm^{-3}, NH_3 mixing ratio, C_{NH3}, of 0.1–100 ppt and J of 10^{-5}–10^{6} cm^{-3} s^{-1} [*Napari et al.*, 2002]. NA02, however, contains a technical flaw, as it only accounts for hydrate formation and neglects the formation of ammonia bisulfate (NH_4HSO_4) and its effect on the nucleation rates. As pointed out by *Yu* [2006b], NA02 significantly overpredicts (by many orders of magnitude) the effect of NH_3 on nucleation when compared with laboratory measurements [e.g., *Ball et al.*, 1999; *Kim et al.*, 1998]. *Yu* [2006b] and *Anttila et al.* [2005] offered two opposite reasons for the overprediction. *Yu* [2006b] argued that NH_3 cannot stabilize small H_2SO_4-H_2O clusters due to a weak molecular bonding between NH_3 and small H_2SO_4 clusters [*Ianni and Bandy*, 1999; *Nadykto and Yu*, 2007] and thus the effect of NH_3 on nucleation is small. In contrast, the theory of *Anttila et al.* [2005] is based on the assumption that the bonding between NH_3 and small H_2SO_4 clusters is so strong that nearly all H_2SO_4 vapor molecules in the atmosphere are bonded to become NH_4HSO_4 [*Vehkamäki et al.*, 2004]. Similar to the effect of H_2SO_4 monomer hydration on nucleation, the formation of NH_4HSO_4 has been shown to significantly reduce the THN rate due to higher energy demands required to form the critical cluster from hydrates than free molecules [*Anttila et al.*, 2005; *Merikanto et al.*, 2007b]. The effect of NH_4HSO_4 formation was considered in ME07, which is valid for atmospheric conditions with $T > 235$ K, RH of 0.05–0.95, N_{H2SO4} of 5×10^{4}–10^{9} cm^{-3}, C_{NH3} of 0.1–1000 ppt and $J > 10^{-5}$ cm^{-3} s^{-1}. *Yu* [2006b] derived a THN kinetic model that uses the laboratory data to constrain the average NH_3 stabilization effect ($F_{NH3} = 2$) in calculating J values. The THN model was derived based on the theory that only a small fraction of small H_2SO_4 clusters contain NH_3 while a large fraction contain water in the atmosphere due to the abundance of atmospheric water [*Kurtén et al.*, 2007; *Nadykto et al.*, 2009].

[11] *Sihto et al.* [2006] derived the prefactors in the power law expressions based the activation and kinetic nucleation theories suggested by *Kulmala et al.* [2006] using observed nucleation rates from field campaigns in Europe. In the cluster-activated nucleation, activation of small clusters is assumed to occur via heterogeneous nucleation or heterogeneous chemical reactions with J directly proportional to N_{H2SO4}. The prefactor A is an empirical coefficient describing the actual physics and chemistry of the nucleation process. In the kinetic nucleation, critical clusters are assumed to form by collisions of H_2SO_4 or other molecules containing H_2SO_4, e.g., NH_4HSO_4, with J proportional to the square of N_{H2SO4}. Prefactor K is related to rate constants for reactions that lead to the production of stable nuclei. Both A and K values are empirically determined from observation-derived nucleation rates as a function of H_2SO_4 concentrations using the method of least squares. Their values may vary with location or season or time of sampling. The cluster-activated nucleation expression of *Sihto et al.* [2006] with a mean prefactor A value of 1.7×10^{-6} and a power of 1 is used in this study. *Kuang et al.* [2008] derived the values of the exponent and the prefactor A or K in the power law expression using several observational data sets. They found that the power law expression with a mean prefactor K value of 1.6×10^{-14} and a P value of 2.01 provides the best fit to the J values in Atlanta observed from the Aerosol Nucleation and Real Time Characterization Experiment (ANARChE) study of nucleation during late July–August 2002 [*McMurry et al.*, 2005]. This kinetic type nucleation expression along with the mean K value is used in this study. Additional simulations using the minimal and maximum A and K reported by *Sihto et al.* [2006] and *Kuang et al.* [2008] are also conducted to study the sensitivity of J to these prefactors.

[12] In this paper, the nucleation rates are calculated using the above 12 nucleation parameterizations under atmospheric conditions with T of 180–303 K, RH of 0–100%,

N_{H2SO4} of 10^4–5×10^{11} cm^{-3}, and C_{NH3} of 0.1–100 ppt that may occur in the atmosphere from polluted surface to very clean mesopause (~80 km above the surface). Those rates are also compared with the maximum possible rates of J_{dimer} and $J_{2\ nm}$. In addition, the calculated J values are compared with laboratory measurements by *Ball et al.* [1999] and evaluated using $J_{1\ nm}$ values derived based on particle size distribution and chemical measurements at Jefferson Street (JST), Atlanta, GA from ANARChE during late July through August 2002 [*McMurry and Eisele*, 2005]. ANARChE was selected because of the availability of J data and the observed nucleation events during this field campaign involved only H_2SO_4 and NH_3 [*Smith et al.*, 2005; *Sakurai et al.*, 2005]. These parameterizations are then evaluated further in the 3-D CMAQ model using observed particle size distributions from the Aerosol Research Inhalation Epidemiological Study (ARIES) [*Van Loy et al.*, 2000] 12–28 during June 1999 [see *Zhang et al.*, 2010].

3. Comparison of Parameterizations Under Hypothetical Atmospheric Conditions

3.1. Dependence of Nucleation Rates on N_{H2SO4}

[13] Figure 1 shows the calculated nucleation rates, J, as a function of N_{H2SO4} on a logarithmic scale. Note that the rates below 10^{-8} cm^3 s^{-1} are too small to have important effects on new particle formation and those above 10^{12} cm^3 s^{-1} are too large to be realistic, they are therefore not shown in Figure 1. The ternary nucleation rates from NA02 and ME07 are calculated at C_{NH3} of 0.1 ppt and 100 ppt to provide a bound of their ternary rates. Those by YU06 do not vary with NH_3 levels, whose effects are considered to be an average enhancement factor derived from laboratory measurements of *Ball et al.* [1999] with C_{NH3} of ~100 ppt. For KU98, VE02, NA02, YU06, ME07, and YU08, only J values in their valid ranges of T, RH, N_{H2SO4}, and J are plotted, although they may give nonzero J values beyond those ranges. The upper limit rates of collision-controlled nucleation in terms of J_{dimer} and $J_{2\ nm}$ are also plotted for comparison.

[14] At the middle tropospheric conditions with RH = 50%, T = 258.15 K, and $N_{H2SO4} = 10^4$–10^{12} cm^{-3} (Figure 1a), all parameterizations show a strong dependence of J on N_{H2SO4} and at a given N_{H2SO4} the values of J predicted by the models can vary by up to 15 orders of magnitude. The dependence of log(J) on log(N_{H2SO4}) can be roughly grouped into three types: strong linear (i.e., PA94, FI98, KU98, YU06, and YU08), weak linear (i.e., WE94, HK98, SI06, and KU08), and nonlinear (i.e., VE02, NA02, and ME07). Among the 7 BHN parameterizations, WE94 gives zero rates for $N_{H2SO4} < 5 \times 10^7$ cm^{-3} and a relatively weaker dependence on N_{H2SO4} for higher N_{H2SO4} values, because J is not directly proportional to N_{H2SO4}, but it is directly proportional to the difference between this and the critical concentration of H_2SO_4 that is required to produce J of 1 cm^{-3} s^{-1}. PA94, FI98, and KU98 show a strong linear dependence of log(J) on log (N_{H2SO4}) that is similar in terms of magnitude but for different ranges of N_{H2SO4} because their log(J) values are directly proportional to log (N_{H2SO4}), with the highest rates by FI98 and the lowest rates by PA94. VE02 shows a strong dependence of log(J) on log(N_{H2SO4}) that is linear for $N_{H2SO4} < 2 \times 10^8$ cm^{-3} but nonlinear for higher N_{H2SO4}. For 10^{-8} cm^3 s^{-1} < J < 10^{15} cm^3 s^{-1}, the rates predicted by KU98 are lower by 1–2 and 4–6 orders of magnitude compared with those of VE02 and FI98, respectively. The differences between rates by KU98 and VE02 can be mainly attributed to differences in their treatment for hydrate formation. HK98 shows a weaker dependence on N_{H2SO4} than other BHM parameterizations except for WE94, due in part to its consideration of the competition between nucleation and condensation that leads to a lower N_{H2SO4} available for nucleation. YU08 shows a strong linear dependence of log(J) on log(N_{H2SO4}). For THN parameterizations, NA02 show a nonlinear dependence of log(J) on log(N_{H2SO4}) at C_{NH3} of 0.1 ppt but a nearly linear dependence at C_{NH3} of 100 ppt. ME07, on the other hand, gives slightly nonlinear dependence of log(J) on log(N_{H2SO4}) at C_{NH3} of 0.1 and 100 ppt. ME07 gives rates that are lower than those of NA02 by up to 11 orders of magnitude at C_{NH3} of 0.1 ppt and by up to 9 orders of magnitude at C_{NH3} of 100 ppt, given the same value of N_{H2SO4} when $N_{H2SO4} < 10^9$ cm^{-3}. YU06 gives J values that are significantly lower than those by NA02 at C_{NH3} = 0.1 and 100 ppt and by ME07 at C_{NH3} = 100 ppt for $N_{H2SO4} < 10^9$ cm^{-3} but higher than J from ME07 at C_{NH3} = 0.1 ppt for the valid N_{H2SO4} and J ranges of ME07, because it uses experimental data to constrain J values. The THN J values predicted by YU06 are within 1 order of magnitude of BHN rates, consistent with laboratory studies [e.g., *Kim et al.*, 1998; *Ball et al.*, 1999]. By comparison, the THN rates from NA02 at C_{NH3} = 100 ppt are 4–15 orders of magnitude higher than rates by all BHM parameterizations for $N_{H2SO4} < 2 \times 10^8$ cm^{-3} (except for WE94 and FI98 at some N_{H2SO4} values), inconsistent with observed enhancement factors for J in the presence of ambient level of NH_3, which is consistent with the finding of *Yu* [2006b]. As pointed previously, *Anttila et al.* [2005] and ME07 attributed such a significant discrepancy to the omission of the formation of NH_4HSO_4 and its effect on the nucleation rates of NA02, but *Yu* [2006b] argued that it is caused by the weak bonding of NH_3 with small H_2SO_4 molecular clusters. The correction made for NA02 shown by ME07 brings the THN J values at C_{NH3} = 100 ppt in a much closer agreement (0–7 orders of magnitude) with the BHN rates, although those by ME07 at C_{NH3} = 0.1 ppt become much lower than the BHN rates for $10^8 \le N_{H2SO4} \le 10^9$ cm^{-3}. For the two power laws, SI06 gives linear dependence of log(J) on log(N_{H2SO4}) similar to WE94 but its rates are valid for a wider range of N_{H2SO4} including those below 5×10^7 cm^{-3}, and KU07 shows a linear dependence of log(J) on log(N_{H2SO4}) that is stronger than WE94, HK98, and SI06 but weaker than those of PA94, FI98, and KU98. SI06 gives higher J than KU08 at $N_{H2SO4} < 10^8$ cm^{-3} but lower one than KU08 for higher N_{H2SO4}, indicating a stronger nucleation simulated by KU08 under a sulfate-rich environment. Compared with J_{dimer} and J_{2nm}, some J values exceed these upper limits, including all rates by NA02 at C_{NH3} > 0.1 ppt, nearly all rates by WE94, and some rates by PA94, FI98, VE02, and NA02 at C_{NH3} = 0.1 ppt at some N_{H2SO4}.

[15] At surface conditions with RH = 80%, T = 298.15 K, and $N_{H2SO4} = 10^4$–10^{12} cm^{-3} (Figure 1b) all BHN and THN parameterizations except those of PA94 predict much lower J than those at RH = 50% and T = 258.15 K, which may

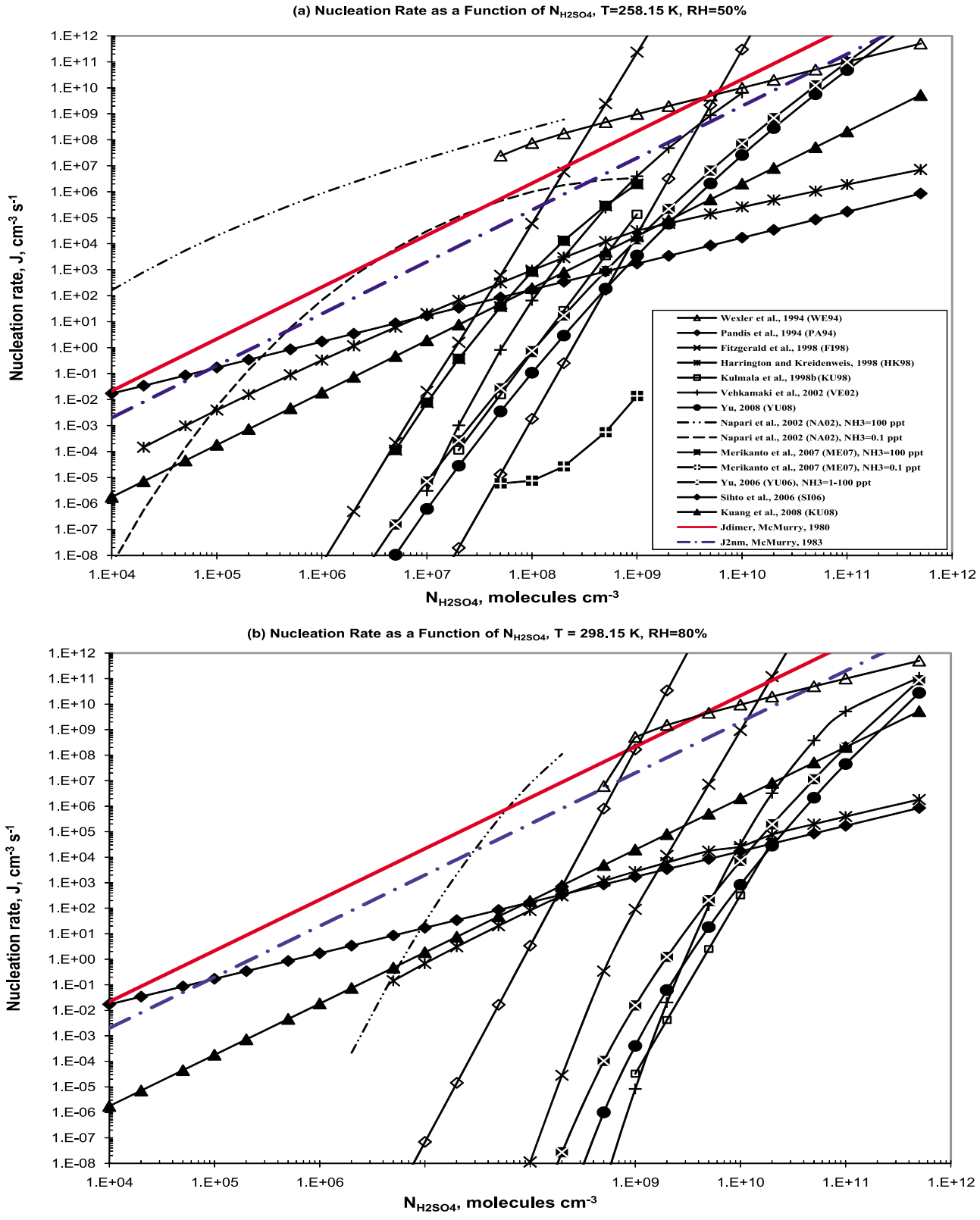

Figure 1. Nucleation rates as a function of the number concentration of H_2SO_4 at (a) T = 258.15 K, RH = 50%, and (b) T = 298.15 K, RH = 80%.

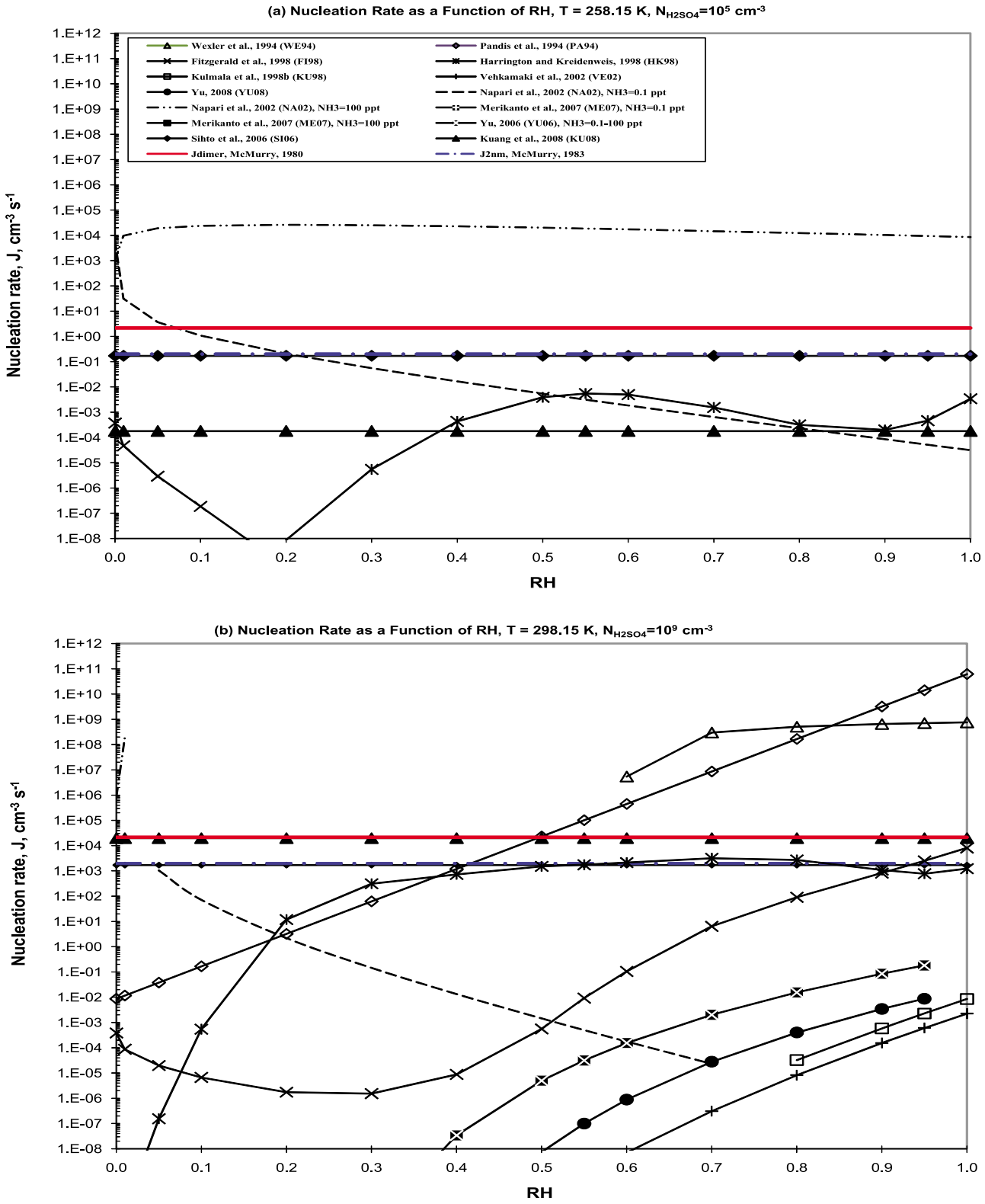

Figure 2. Nucleation rates as a function of temperature at (a) RH = 50%, and the number concentration of H_2SO_4 of 10^5 molecules cm^{-3}, and (b) RH = 80%, and the number concentration of H_2SO_4 of 10^9 molecules cm^{-3}.

vary by up to 18 orders of magnitude at the same N_{H2SO4}. Since J values generally increase when RH increases from 50% to 80% and decrease when T increases from 258.15 K to 298.15 K (with a few exceptions; see Figures 2 and 3), the increases in J values under the surface conditions indicate that the effect of T variation dominates over that of RH

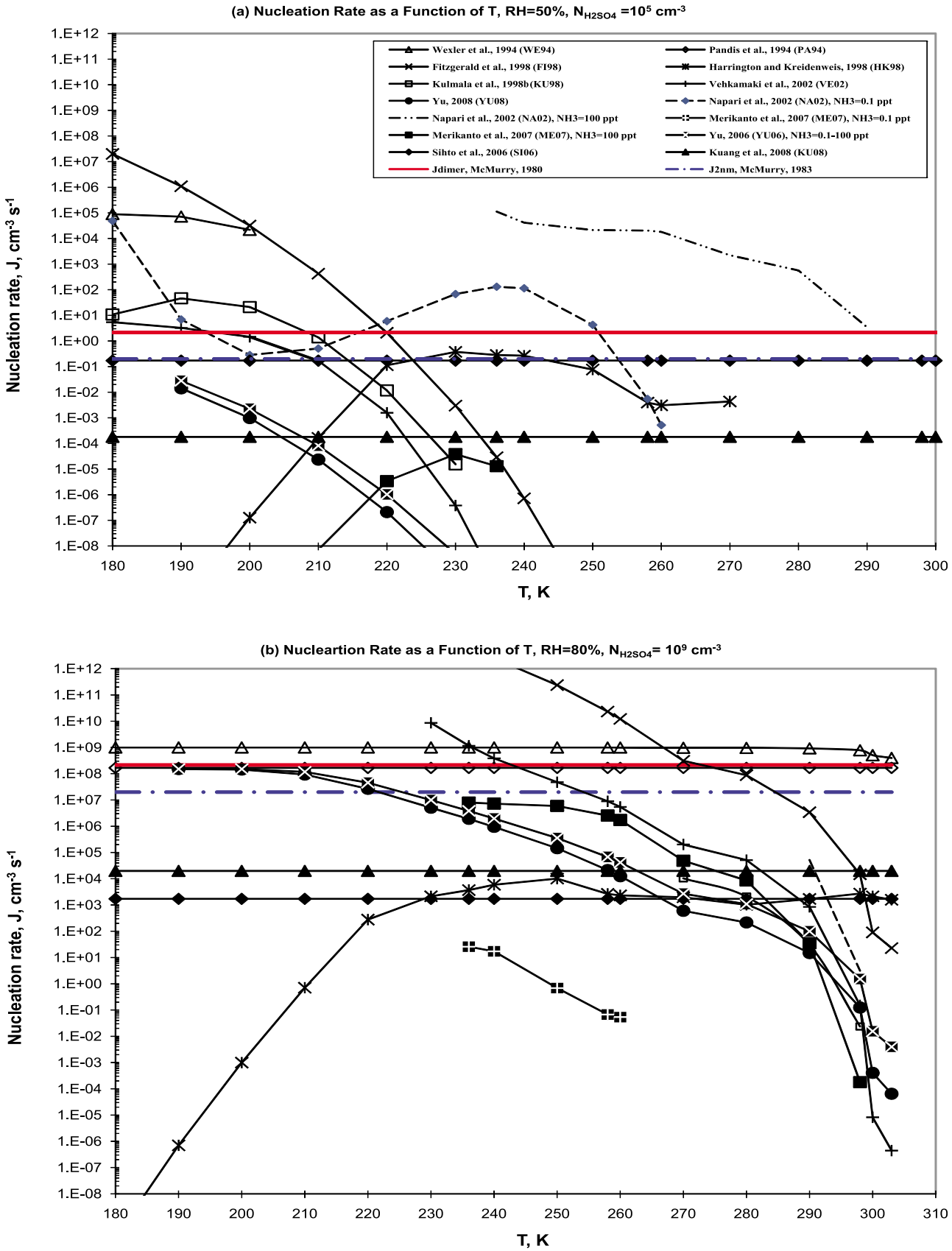

Figure 3. Nucleation rates as a function of RH at (a) T = 258.15 K, and the number concentration of H_2SO_4 of 10^5 molecules cm^{-3}, and (b) T = 298.15 K, and the number concentration of H_2SO_4 of 10^9 molecules cm^{-3}.

variation, as compared with those under the middle tropospheric conditions. WE94 shows a similar strong dependence of log(J) on log(N_{H2SO4}) but with rates that are lower by up to 100% than RH = 50% and T = 258.15 K at $N_{H2SO4} > 5 \times 10^8$ cm^{-3} and predicts no nucleation for lower N_{H2SO4}. FI98 and KU08 give rates that are lower by 9–12 and 10 orders of magnitude, respectively, at RH = 80% and T = 298.15 K than RH = 50% and T = 258.15 K. VE02 does not give a rate that is greater than 10^{-8} cm^{-3} s^{-1} at $N_{H2SO4} < 6 \times 10^8$ cm^{-3} and gives rates that are lower by 3–12 orders of magnitude at RH = 80% and T = 298.15 K than RH = 50% and T = 258.15 K at higher N_{H2SO4} levels. YU08 gives similar dependence of log(J) on log(N_{H2SO4}) but with rates that are lower by 7–22 orders of magnitude under the surface conditions than the middle tropospheric conditions. PA04 also shows a similar strong dependence of log(J) on log(N_{H2SO4}) to that at a lower RH (note that it does not depend on T), but it depends on RH to a much lesser extent than N_{H2SO4} with rates of 1–4 orders of magnitude higher at RH = 80% than those at RH = 50%. At C_{NH3} = 100 ppt, NA02 gives much stronger dependence of log(J) on log(N_{H2SO4}) with rates that are lower by 1–10 orders of magnitude under the surface conditions than the middle tropospheric conditions for $N_{H2SO4} < 5 \times 10^8$ cm^{-3}. At C_{NH3} = 0.1 ppt, it gives either zero rates at $N_{H2SO4} < 5 \times 10^5$ cm^{-3} or rates that are less than its low limit of validation value (i.e., 10^{-5} cm^{-3} s^{-1}) at higher N_{H2SO4} (thus not shown in the Figure 1b). Compared with J values under the middle tropospheric conditions, ME07 predicts no nucleation at C_{NH3} = 0.1 and 100 ppt (thus not shown in the Figure 1b). Relative to the BHN rates by YU08, YU06 shows larger NH_3 enhancement factors under the surface conditions than those under the middle tropospheric conditions, but they are within 2 orders of magnitude and remain consistent with laboratory studies. Some rates simulated by WE94, FI98, PA94, and NA02 at C_{NH3} > 0.1 ppt exceed the upper limits (J_{dimer} and J_{2nm}). Under the surface conditions, SI06 and KU08 show the same N_{H2SO4} dependence and the same J values as those under the middle tropospheric conditions, because they do not depend on T and RH.

3.2. Dependence of Nucleation Rates on *T*

[16] Figures 2a and 2b show J as a function of T on a semilogarithmic scale at RH = 50% and $N_{H2SO4} = 10^5$ cm^{-3} and RH = 80% and $N_{H2SO4} = 10^9$ cm^{-3}, respectively. At RH = 50% and $N_{H2SO4} = 10^5$ cm^{-3}, PA94 and ME07 give either negligible nucleation rates or do not predict nucleation. WE94 does not predict nucleation when T > 200 K. The calculated J values are above 10^{-8} cm^{-3} s^{-1} for YU06 and YU08 when $T < 230$ K, for VE02 and KU98 when $T < 235$ K, and for FI98 when $T < 245$ K. Only HK98, SI06, KU08, and NA02 give valid J values (defined as values that are within their respective valid ranges and also $\leq J_{2\ nm}$) for T > 250 K. While rates by SI06 and KU08 do not depend on T, those by FI98, HK98, YU08, YU06, and NA02 show a strong nonlinear dependence of log(J) on T. The rates given by all parameterizations generally decrease with T except those from HK98 that increase with T for T < 230 K and those from NA02 with C_{NH3} = 0.1 ppt that oscillates with T. The J values simulated by these parameterizations may vary by up to 15 orders of magnitude when T increases from 180 to 235 K (i.e., FI98) and by 5 orders of magnitude when T increases from 240 to 290 (i.e., NA02 at C_{NH3} = 0.1 ppt). At the same T, the J values from various parameterizations may differ by 13 orders of magnitude for $J > 10^{-8}$ cm^{-3} s^{-1}. Some rates by WE04, KU98, FI98, and NA02 are much higher than J_{dimer} and $J_{2\ nm}$. SI06 gives a constant rate of 0.17 cm^{-3} s^{-1}, which is lower than J_{dimer} of 2.15 cm^{-3} s^{-1} and $J_{2\ nm}$ of 0.2 cm^{-3} s^{-1}. KU08 gives a constant rate of 1.8×10^{-4} cm^{-3} s^{-1}, which is well below J_{dimer} and $J_{2\ nm}$.

[17] At RH = 80% and $N_{H2SO4} = 10^9$ cm^{-3}, NA02 only gives two valid J values between 10^{-5}–10^6 cm^{-3} s^{-1} at C_{NH3} = 0.1 ppt and T = 290 and 298 K and gives all J values that are larger than 10^6 cm^{-3} s^{-1} at C_{NH3} = 100 ppt (thus not shown in Figure 2b). WE94, PA94, SI06, and KU08 show either no or weak T dependence, the remaining parameterizations show a strong T dependence, with rates by KU98, FI98, VI02, YU08, YU06, and ME07 decreasing with T but those by HK98 increasing with T at lower T values but decreasing with T or remaining nearly constant at higher T values after reaching a peak J value. The J values simulated by these parameterizations may change by up to 12 orders of magnitude when T increases from 185 to 250 K (i.e., HK98) and by up to 16 orders of magnitude when T increases from 230 to 303 K (i.e., VE02), indicating a very strong T dependence. At the same T, the J values from various parameterizations may differ by 17 orders of magnitude at T < 260 K and by 15 orders of magnitude at higher T values for $J > 10^{-8}$ cm^{-3} s^{-1}. Several parameterizations give rates much higher than J_{dimer} of 2.2×10^8 cm^{-3}s^{-1} and $J_{2\ nm}$ of 2×10^7 cm^{-3}s^{-1} including those of WE94 at all T values, FI98 at T < 290 K, and VI02 at T < 250 K. PA94 gives a constant rate of 1.7×10^8 cm^{-3} s^{-1}, which is slightly below J_{dimer} but about 1 order of magnitude higher than $J_{2\ nm}$. KU08 and SI06 give constant rates of 1.9×10^4 and 1.7×10^3 cm^{-3} s^{-1}, respectively, which are well below J_{dimer} and $J_{2\ nm}$.

3.3. Dependence of Nucleation Rates on *RH*

[18] Figures 3a and 3b show the J values on a semilogarithmic scale as a function of RH at the middle tropospheric conditions with T = 258.15 K and $N_{H2SO4} = 10^5$ cm^{-3} and the urban surface conditions with T = 298.15 K and $N_{H2SO4} = 10^9$ cm^{-3}. Under the middle tropospheric conditions, WE94, PA94, VE02, KU98, HK98, YU06, ME07, and YU08 do not predict nucleation. SI06, KU08, and NA02 at C_{NH3} = 100 ppt show either no or weak RH dependence. FI98, HK98, and NA02 at C_{NH3} = 0.1 ppt show stronger RH dependence with rates that vary by up to 8 orders of magnitude when RH increases from 0.01% to 100% for $J > 10^{-8}$ cm^{-3}s^{-1}. Simulated J values by NA02 at C_{NH3} = 100 ppt are higher by up to 12 orders of magnitude than those from the binary parameterizations at the same RH value for $J > 10^{-8}$ cm^{-3}s^{-1}. The rates by FI98 and NA02 at C_{NH3} = 0.1 ppt for all RH values and NA02 at C_{NH3} = 100 ppt when RH > 20% decrease with RH, and those by HK98 can change in either way depending on RH. The RH dependence simulated by FI98 and NA02 is inconsistent with laboratory observations of *Kim et al.* [1998] and *Ball et al.* [1999], consistent with finding of *Yu* [2006b]. NA02 gives J values that are well above J_{dimer} of 2.2×10^{-2} cm^{-3}s^{-1} and $J_{2\ nm}$ of 2.0×10^{-3} cm^{-3}s^{-1} when C_{NH3} = 100 ppt and sometimes above

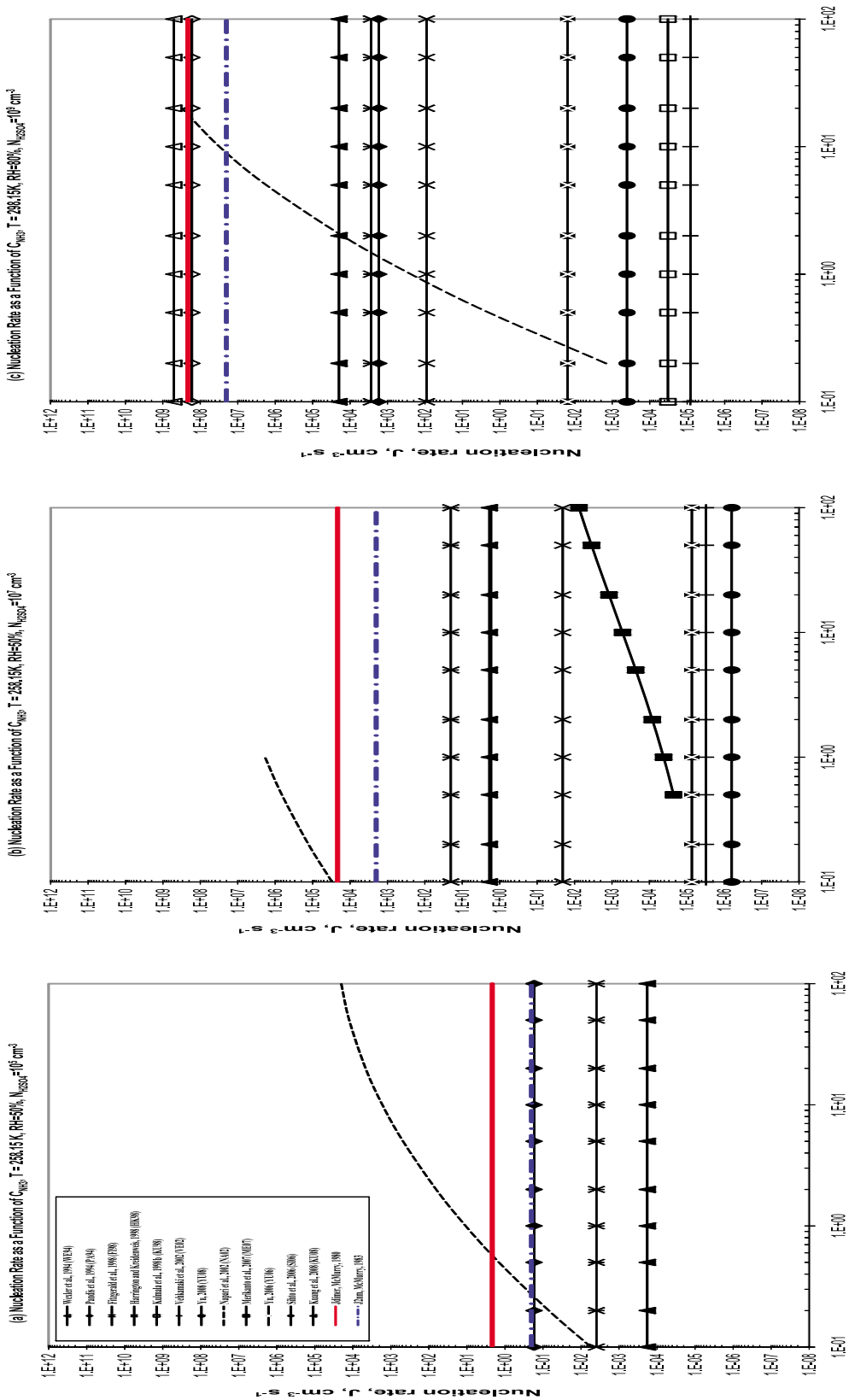

Figure 4. Nucleation rates as a function of the mixing ratio of NH3 at (a) T = 258.15 K, RH = 50%, and the number concentration of H_2SO_4 of 10^5 molecules cm^{-3}, (b) T = 258.15 K, RH = 50%, and the number concentration of H_2SO_4 of 10^7 molecules cm^{-3}, and (c) T = 298.15 K, RH = 80%, and the number concentration of H_2SO_4 of 10^9 molecules cm^{-3}.

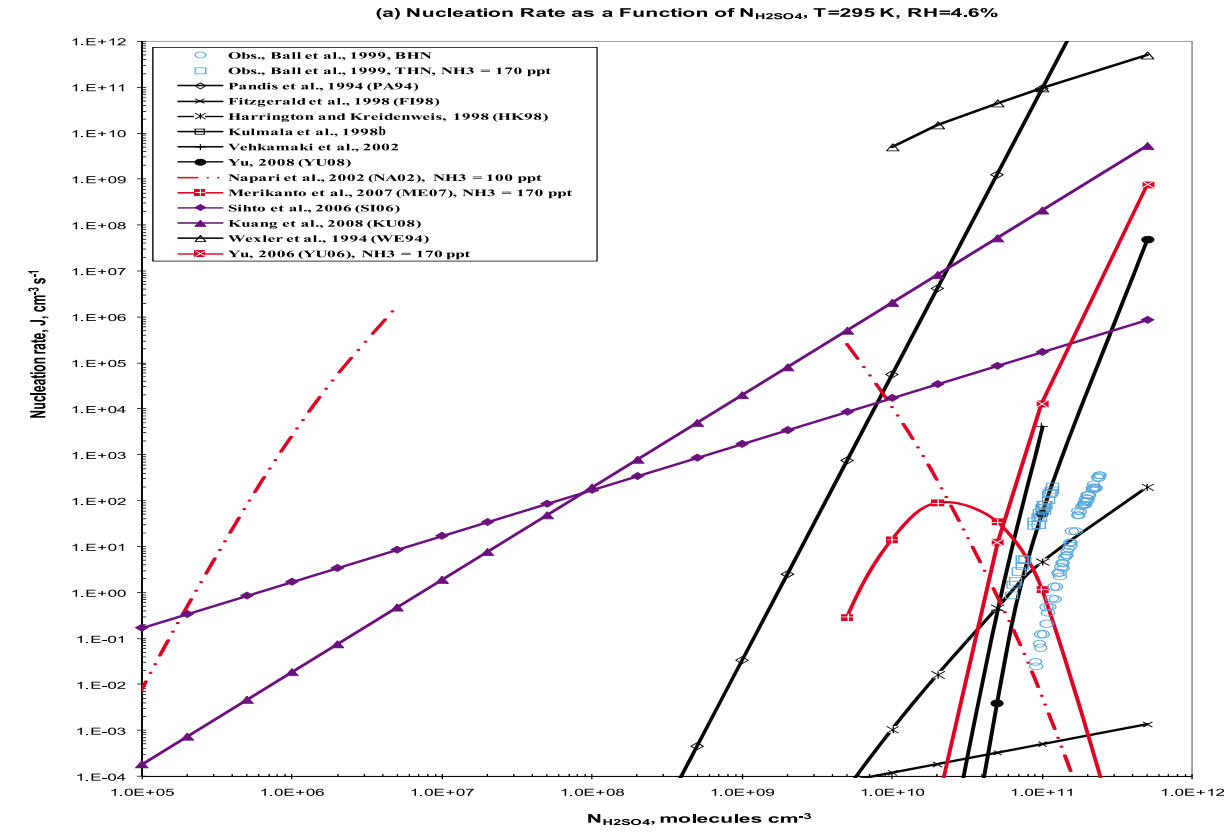
(a) Nucleation Rate as a Function of N_{H2SO4}, T=295 K, RH=4.6%
Obs., Ball et al., 1999, BHN
Obs., Ball et al., 1999, THN, NH3 = 170 ppt
Pandis et al., 1994 (PA94)
Fitzgerald et al., 1998 (FI98)
Harrington and Kreidenweis, 1998 (HK98)
Kulmala et al., 1998b
Vehkamaki et al., 2002
Yu, 2008 (YU08)
Napari et al., 2002 (NA02), NH3 = 100 ppt
Merikanto et al., 2007 (ME07), NH3 = 170 ppt
Sihto et al., 2006 (SI06)
Kuang et al., 2008 (KU08)
Wexler et al., 1994 (WE94)
Yu, 2006 (YU06), NH3 = 170 ppt
Nucleation rate, J, cm^{-3} s^{-1}
1.E+12
1.E+11
1.E+10
1.E+09
1.E+08
1.E+07
1.E+06
1.E+05
1.E+04
1.E+03
1.E+02
1.E+01
1.E+00
1.E-01
1.E-02
1.E-03
1.E-04
1.0E+05
1.0E+06
1.0E+07
1.0E+08
1.0E+09
1.0E+10
1.0E+11
1.0E+12
N_{H2SO4}, molecules cm^{-3}

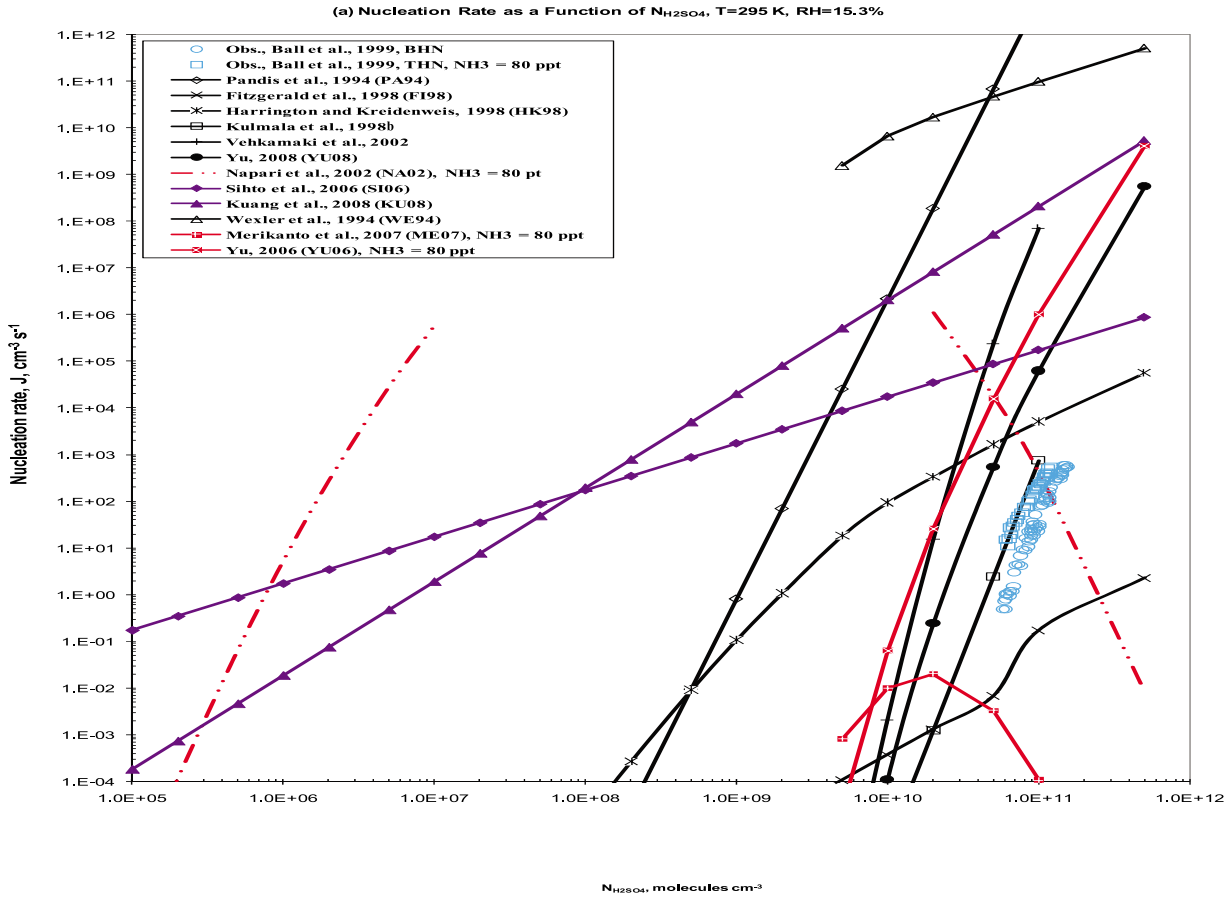
(a) Nucleation Rate as a Function of N_{H2SO4}, T=295 K, RH=15.3%
Obs., Ball et al., 1999, BHN
Obs., Ball et al., 1999, THN, NH3 = 80 ppt
Pandis et al., 1994 (PA94)
Fitzgerald et al., 1998 (FI98)
Harrington and Kreidenweis, 1998 (HK98)
Kulmala et al., 1998b
Vehkamaki et al., 2002
Yu, 2008 (YU08)
Napari et al., 2002 (NA02), NH3 = 80 pt
Sihto et al., 2006 (SI06)
Kuang et al., 2008 (KU08)
Wexler et al., 1994 (WE94)
Merikanto et al., 2007 (ME07), NH3 = 80 ppt
Yu, 2006 (YU06), NH3 = 80 ppt
Nucleation rate, J, cm^{-3} s^{-1}
1.E+12
1.E+11
1.E+10
1.E+09
1.E+08
1.E+07
1.E+06
1.E+05
1.E+04
1.E+03
1.E+02
1.E+01
1.E+00
1.E-01
1.E-02
1.E-03
1.E-04
1.0E+05
1.0E+06
1.0E+07
1.0E+08
1.0E+09
1.0E+10
1.0E+11
1.0E+12
N_{H2SO4}, molecules cm^{-3}

Figure 5

those limits when C_{NH3} = 0.1 ppt, thus not realistic. FI98, HK98, SI06 and KU08 give J values that are lower than J_{dimer} and $J_{2\ nm}$.

[19] Under the urban surface conditions, ME07 does not predict nucleation and NA02 at C_{NH3} = 100 ppt gives J values above 10^9 $cm^{-3}s^{-1}$ that are beyond its valid range (thus no values are shown for those parameterizations). WE94, SI06, and KU08 show either no or weak RH dependence. KU98, PA94, FI98, HK98, VE02, YU06, YU08, and NA02 at C_{NH3} = 0.1 ppt show a strong RH dependence of log(J), with rates that vary by up to 12 orders of magnitude when RH increases from 0.0 to 100% for $J > 10^{-8}$ cm^{-3}. Simulated J values can vary by up to 14 orders of magnitude at the same RH value for $J > 10^{-8}$ cm^{-3}. The rates by all these parameterizations increase with RH except those by NA02 at C_{NH3} = 0.1 ppt that decrease with RH and those by FI98 that decrease with increased RH from 0 to 30% but increase with increased RH when RH further increases to 100%. As indicated previously, the RH dependence simulated by NA02 and FI98 at RH < 30% is inconsistent with laboratory observations and other nucleation parameterizations. All rates by WE94 and some rates by PA94 at RH > 50% and FI98 at RH > 0.95 exceed J_{dimer} and $J_{2\ nm}$, thus not realistic. KU08 and SI06 give a constant rate of 2.0×10^4 $cm^{-3}s^{-1}$ and 1.7×10^3 $cm^{-3}s^{-1}$, respectively, which is slightly lower than J_{dimer} of 2.2×10^4 $cm^{-3}s^{-1}$ and $J_{2\ nm}$ of 2.0×10^3 $cm^{-3}s^{-1}$, respectively.

3.4. Dependence of Nucleation Rates on C_{NH3}

[20] Figures 4a–4c show J as a function of C_{NH3} on a logarithmic scale at the middle tropospheric conditions with RH = 50%, T = 258.15 K, and N_{H2SO4} of 10^5 and 10^7 cm^{-3} and urban surface conditions with RH = 80%, T = 298.15 K, and N_{H2SO4} of 10^9 cm^{-3}, respectively. Under the middle tropospheric conditions with RH = 50%, T = 258.15 K, and N_{H2SO4} of 10^5 cm^{-3}, WE94 does not predict nucleation, HK98 gives a rate of 3.9×10^{-3} cm^{-3} s^{-1}, and the rest of binary parameterizations all give rates that are negligible ($<10^{-15}$ cm^{-3} s^{-1}) (not shown in Figure 4). Among the three THN parameterizations, ME02 does not predict nucleation, YU06 gives negligible rates, and only NA02 predicts J values that are above 10^{-8} cm^{-3} s^{-1}, which increase by more than 7 orders of magnitude when C_{NH3} increases from 0.1 to 100 ppt for $J > 10^{-8}$ cm^{-3} s^{-1}. These rates are higher than J values by SI06 and KU08 at C_{NH3} > 2.2 ppt and 0.1 ppt, respectively, and those by all BHN parameterizations when C_{NH3} = 0.1–100 ppt. NA02 at C_{NH3} > 0.5 or 0.2 ppt gives rates that are higher than J_{dimer} or $J_{2\ nm}$, respectively. When N_{H2SO4} increases from 10^5 cm^{-3} to 10^7 cm^{-3} in the troposphere (i.e., corresponding to cases with volcanic eruptions during which high SO_2 amounts are emitted, leading to a high N_{H2SO4} in the upper/middle troposphere), the J values simulated from all parameterizations increase by several orders of magnitude because their positive dependence on N_{H2SO4} and all parameterizations give rates above 10^{-8} cm^{-3} s^{-1} except for WE94, which does not predict nucleation, PA94, which gives a negligible rate of 1.4×10^{-10} cm^{-3} s^{-1}, and KU98, which gives a rate of 2.7×10^{-6} cm^{-3} s^{-1} that is beyond its valid range of J (both PA94 and KU98 predictions are thus not shown in Figure 4b) The J values from NA02 are higher by 11 orders of magnitude than those from ME07 and YU06, 3–12 orders of magnitude than those from binary parameterizations, and 5–6 orders of magnitude than those from power law parameterizations. While the J values from NA02 exceed J_{dimer} and $J_{2\ nm}$, those from all other parameterizations are well below these limits. At urban surface conditions, ME07 does not predict new particle formation. NA02 shows a strong C_{NH3} dependence with rates increasing by 11 orders of magnitude when C_{NH3} increases from 0.2 to 20 ppt. YU06 gives a constant rate of 1.6×10^{-2} cm^{-3} s^{-1}, which is higher than the corresponding binary rate of 4.0×10^{-4} cm^{-3} s^{-1} by YU08. KU98, VE02, and YU08 give rates that are lower than ternary rates by YU06 and NA02 for all C_{NH3} values. The rest of binary and power law parameterizations give rates that are higher than those by YU06 for all C_{NH3} values and higher than those by NA02 at lower NH_3 levels but lower values at higher NH_3 levels. Among all parameterizations, WE94 gives the highest rates and VE02 gives the lowest rates. The rates by WE94, PA04, and NA02 at C_{NH3} > 10 ppt are higher than J_{dimer} or $J_{2\ nm}$, thus not realistic.

4. Evaluation of Parameterizations Using Laboratory Measurements

[21] *Yu* [2006b] has previously evaluated J rates calculated by NA02 and VE02 with the laboratory data of *Ball et al.* [1999]. A similar comparison for all 12 nucleation parameterizations using the same laboratory data is shown in Figure 5 (note that only results under their respective valid conditions are plotted). Under the conditions with T = 295 K and RH = 4.6%, the measured BHN and THN rates range from 3.1×10^{-2} to 3.6×10^2 cm^{-3} s^{-1} and 9.0×10^{-1} to 2.0×10^2 cm^{-3} s^{-1}, respectively. The measured nucleation rates are enhanced in the presence of 170 ppt NH_3 by roughly 2–3 orders of magnitudes. For comparison, WE04 and PA98 give J values that are higher by up to 10 orders of magnitude, FI98 gives J values that are lower by 2 orders of magnitude, VE02 gives negligible J values, and KU98 is not valid for RH < 10% (off scale in Figure 5). Among all BHN parameterizations, YU08 and HK98 give the closest agreement with measured BHN rates. Among ternary parameterizations, YU06 gives the closest agreement, ME07 does not predict nucleation (off scale in Figure 5), and NA02 gives rates of 10^{-2} to

Figure 5. Simulated versus measured nucleation rates under the laboratory conditions with (a) T = 295 K and RH = 4.6% and (b) T = 295 K and RH = 15.3%. The symbols in blue are experimental data from *Ball et al.* [1999]. The lines in black, red, and purple represent parameterizations based on binary homogeneous nucleation (BHN), ternary homogeneous nucleation (THN), and empirical power laws, respectively. The results from each parameterization are plotted for their receptive valid ranges of conditions. Note that KU98 data are invisible in Figure 5a because the results are invalid under such a condition and ME07 data are invisible in Figures 5a and 5b because the study does not predict nucleation under such conditions.

10^6 cm^{-3} s^{-1} when $N_{H2SO4} < 1.0 \times 10^9$ cm^{-3} and is invalid for high values of N_{H2SO4}. At the same values of N_{H2SO4}, NA02 gives J values that are up to several tens of orders of magnitude higher than those of KU98 and VE02. For example, the J values are 5.5×10^4 cm^{-3} s^{-1} for NA02, 5.6×10^{-43} cm^{-3} s^{-1} for KU98, and 0 for VE02 when $N_{H2SO4} = 2.0 \times 10^6$ cm^{-3}. Such a dramatic enhancement in nucleation rates in the presence of NH_3 was not observed in the laboratory experiments. The two power laws give J values that are higher by up to 6–8 orders of magnitude than measured BHN and THN rates, which is expected because those power laws were derived based on ambient atmospheric measurements obtained under different conditions from laboratory measurements. For example, SI06 law was derived from observations under T of 266–280 K, and RH of 43–93% in springtime in Hyytiälä, Finland [*Kulmala et al.*, 2001b; *Boy et al.*, 2005], and KU08 law was derived from observations under T of 301.5–310.7 K and RH of 35–76% during summertime in Atlanta, Georgia [*Kuang et al.*, 2008]. Under the conditions with T = 295 K and RH = 15.3%, the results for all above parameterizations except for KU98 and their relative differences and deviations from laboratory data are similar to those at T = 295 K and RH = 4.6%. Unlike the previous case, KU98 gives the closest agreement with measured BHN rates despite the mistakes in its derivation, and VE02 gives J rates of 10^{-4} to 10^8 cm^{-3} s^{-1} when $N_{H2SO4} > 10^{10}$ cm^{-3}. HK98, YU08, and YU06 deviate further from the laboratory data when RH increases from 4.6% to 15.3%. While the enhancement factor becomes smaller (within 1–2 orders of magnitude) as RH increases, the significant differences between the THN rates by NA02 and the BHN rates by KU98 and VE02 remain similar. These findings are consistent with those of *Yu* [2006b].

[22] Auxiliary material Figures S1–S5 compare simulated nucleation rates with additional measured nucleation rates (or calculated nucleation rates based on measured particle number concentrations) in recent laboratory studies including those by *Berndt et al.* [2005, 2006], *Berndt et al.* [2010], *Young et al.* [2008], *Benson et al.* [2009], and *Sipilä et al.* [2010], respectively.[1] The experimental conditions for all laboratory and field measurements used in this study are summarized in auxiliary material Table S1. It is noted that all these data were obtained from laboratory experiments that generated H_2SO_4 from the SO_2 + OH reactions. Strictly speaking, these measurements are different from previous data obtained using the liquid samples of H_2SO_4 [e.g., *Ball et al.*, 1999]. They do not represent the H_2SO_4-H_2O binary nucleation (instead, it is the H_2SO_4-H_2O-X ternary nucleation, where X is an unidentified species and has been speculated to be an organic species or HSO_5 [*Berndt et al.*, 2005, 2008]. As shown by *Berndt et al.* [2008] and *Sipilä et al.* [2010], those new data using H_2SO_4 from the SO_2 + OH reactions are generally consistent with previously measured data using liquid samples of H_2SO_4. Nevertheless, these newly measured data are useful to evaluate the 12 nucleation parameterizations despite the difference between the type of nucleation observed in various laboratories and the simulated nucleation using various parameterizations and some uncertainties in the "residual" H_2SO_4 and "apparent" nucleation rates in these new laboratory studies [e.g., *Young et al.*, 2008; *Berndt et al.*, 2010].

[23] *Berndt et al.* [2005] and *Berndt et al.* [2006] measured the particle number concentrations in the presence and absence of hydrocarbon, respectively, under a T of 293 K and a range of RH conditions (11–49.5% and 11–60%, respectively). They found a small impact of organics on the formation of H_2SO_4/H_2O particles and estimated a nucleation rate of 0.3–0.4 cm^{-3} s^{-1} for a concentration of H_2SO_4 of ~10^7 cm^{-3}. The nucleation rates shown in auxiliary material Figure S1 are estimated using a residence time of 290 s following the approach of *Berndt et al.* [2005]. However, not all nucleated particle were detectable due to the insufficient counting efficiency of ultrafine condensation particle counter (i.e., TSI_3025) and the loss of H_2SO_4 during those experiments may be high [*Berndt et al.*, 2010]. These estimated J, therefore, represent a lower limit of the actual values due to the uncertainties in the laboratory measurements. As shown in auxiliary material Figure S1, the derived nucleation rates from *Berndt et al.* [2005, 2006] are on the order of 10^{-2} to 10^2 cm^{-3} s^{-1} under various RH conditions. Among the 12 parameterizations, KU08 and SI06 give the closest agreement to the derived nucleation rates (generally within 2 orders of magnitudes). HK98 give rates within 2–3 orders of magnitudes under some conditions (e.g., RH = 42 and 60%). All other parameterizations either do not predict J or give rates that are lower than 1×10^{-8} cm^{-3} s^{-1} (except for FI98 and PA94 under some conditions). Using a high-efficiency particle counter, *Berndt et al.* [2010] recently obtained more reliable J based on more accurate experiments than their previous studies. As shown in auxiliary material Figure S2, the measured nucleation rates are in the range of 0.17–1136, 2.5–335, and 1.5–484 cm^{-3} s^{-1} at T = 293 K and RH values of 22, 45, and 61%, respectively. Those values are indeed higher than derived J of *Berndt et al.* [2005, 2006] that are in the range of 0.02–12, 0.01–81, 0.04–310, 0.02–263, 0.05–52, and 0.02–148 cm^{-3} s^{-1} at RH values of 11%, 19–22%, 42%, 49.5%, and 60%, respectively, indicating a higher accuracy from *Berndt et al.* [2010] than previous measurements. Among the 12 parameterizations, SI06 and KU08 give a good agreement (within 1 order of magnitude) to these newly observed rates, with a closer agreement to them as compared with the earlier measurements of *Berndt et al.* [2005, 2006]. The performance of other parameterizations remains similar or even worse than that under the experimental conditions of *Berndt et al.* [2005, 2006].

[24] As shown in auxiliary material Figure S3, *Young et al.* [2008] measured J under T of 288 K, various RH conditions, as well as other experimental conditions. The flow residence time (tr), wall loss factor (WLF) of H_2SO_4, and the number of H_2SO_4 in the critical cluster are different in these experiments (note that these factors show some impacts on the measured nucleation rates, although they are not explicitly accounted for in the nucleation parameterizations tested here). Auxiliary material Figure S3 shows a large range of simulated J (by >18 orders of magnitudes) from various parameterizations, with the best

[1] Auxiliary materials are available in the HTML. doi:10.1029/2010JD014150.

agreement by HK98 under conditions with T = 288 K, RH = 15%, t_r = 19 s, WLF = 2.4–2.5, and n = ~7 (Figure S3b) and T = 288 K, RH = 11%, t_r = 19 s, WLF = 2.5–2.6, and n = 3–6 (Figure S3c). At T = 288 K, RH = 23%, t_r = 19 s, WLF = 2.4, and n = ~3 (Figure S2a), HK98 and SI06 give values within 4 orders of magnitudes for all H_2SO_4 concentrations, and several parameterizations including those of PA94, VE02, YU06, and YU08 for some H_2SO_4 concentrations. Under most conditions (e.g., auxiliary material Figures S3c–S3e), only a few parameterizations (e.g., KU08, SI06, PA94, HK98, and FI98) give values higher than 1×10^{-8} cm^{-3} s^{-1}.

[25] *Benson et al.* [2009] measured J with and without NH_3 under T = 288 K and RH of 23–33% (indicated by THN and BHN, respectively in auxiliary material Figure S4). They reported an enhancement factor up to ~1000 for NH_3 concentrations of 10–50 ppb. As shown in Figure S4, in the absence of NH_3 (Figures S4a–S4c), SI06 and HK98 give the closest agreement to the measurements. In the presence of NH_3 (Figures S4d–S4f), SI06 and HK98 also give the closest agreement at RH = 23 and 28% and KU08, SI06, and HK98 give the closest agreement at RH = 33%, whereas none of the THN parameterizations give the rates that are within 2–3 orders of magnitudes. NA02 gives rates that are higher by 6–10 orders of magnitudes than the measured rates. ME07 and YU08 give rates that are lower by >7 orders and >9 orders of magnitudes than the measured rates.

[26] As shown in auxiliary material Figure S5, *Sipilä et al.* [2010] measured J with different residence times at 293 K and RH = 22%. The observed rates are in the range of 1–1958 cm^{-3} s^{-1}. SI08 and KU08 show the best agreement to the observed J among all observational data set used for evaluation. HK98, PA94, and FI98 give values that are lower by at least 4, 5, and 9 orders of magnitude than the observed rates, respectively. All other parameterizations either do not predict J or give values that are too small to be significant (<1×10^{-8} cm^{-3} s^{-1}) under such conditions.

5. Evaluation of Parameterizations Using Observations From ANARChE

[27] The above parameterizations are evaluated using observations at Jefferson Street (JST), Atlanta, Georgia, from ANARChE during late July through August 2002. JST is located about 4 km northwest of downtown Atlanta where SO_2 concentrations are high, providing a rich source of H_2SO_4 for new particle formation in an urban environment. The nucleation-related measurements include the mixing ratios of several gases (e.g., SO_2, H_2SO_4, and NH_3), particle size distributions in several size ranges (e.g., 3–40 nm, 20–250 nm, and 0.1–2 μm), and other properties of nanoparticles (e.g., the volatility, hygroscopicity, and chemical composition) [*McMurry and Eisele*, 2005, and references therein]. Since the minimal measurable particle size was ~3 nm for the instruments used during ANARChE, the formation rate of 3 nm particles ($J_{3\ nm}$), can be derived based on the observed particle size distributions and H_2SO_4 number concentrations, and the formation rate of 1 nm particles ($J_{1\ nm}$) can then be extrapolated from $J_{3\ nm}$ [*Kuang et al.*, 2008]. Compared with $J_{3\ nm}$, $J_{1\ nm}$ represents the net nucleation rate of particles with size of 1 nm by accounting for the changes (loss or gain) of particle number concentrations through a combination of several processes including nucleation, condensation, and coagulation in the real atmosphere. It, however, does not account for the formation of particles with size below 1 nm due to these processes (note that instruments developed up to date cannot measure particles <1 nm [see *McMurry et al.*, 2010]). While the observed T, RH, and N_{H2SO4} are available every minute during July–September 2002, the derived values of $J_{1\ nm}$, however, are only available every 2 or 3 min during 0900–1150 Local Daylight Time (LDT), 31 July 2002 and 1110–1305 LDT, 5 August 2002. The two time periods are therefore selected for evaluation of various nucleation parameterizations. The observed T, RH, and N_{H2SO4} data at a 1 min frequency during the two time periods are aggregated into a 2 or 3 min frequency based on that for the derived $J_{1\ nm}$ and then used as the input conditions. The ranges of T, RH, and N_{H2SO4} are 28.32–34.92°C (301.47–308.07 K), 56.83–76.41%, 4.25×10^7–3.03×10^8 cm^{-3}, with mean values of 31.76°C (i.e., 304.91 K), 65.53%, and 1.62×10^8 cm^{-3}, respectively, during 0900–1150 LDT, 31 July 2002, and 34.42–37.58°C (307.57–310.73 K), 34.7–45.5%, 3.42×10^7–2.18×10^8 cm^{-3}, with mean values of 35.95°C (i.e., 309.1 K), 40.42%, and 7.68×10^7 cm^{-3}, respectively, during 1110–1305 LDT, 5 August 2002. 31 July 2002 represents conditions with relatively high N_{H2SO4}, low T, and high RH, and 5 August 2002 represents conditions with relatively low N_{H2SO4}, high T, and low RH. The mean T values of 304.91 K on 31 July and 309.1 K on 5 August are slightly above the valid upper limits of T for some parameterizations (e.g., 298.15 K for KU98, 300 K for NA02, and 305.15 K for VE02). Because the J values from KU98, NA02, and VE02 decrease with increasing T (see Figure 2b), the J values at T = 304.91 and 309.1 K predicted by KU98, NA02, and VE02 should indeed be lower than those at their upper limits of T if the parameterizations are extended at T higher than their upper limits following their T dependence trends (although these values may be often set to be the same at their upper limit of T in their actual 3-D model applications). The actual observed mean T values of 304.91 and 309.1 K are therefore used in calculating J values from KU98, NA02, and VE02 here, which are lower than the J values at their upper limits in 3-D applications. The observed C_{NH3} values range from 1 to 10 ppb during ANARChE [*Nowak et al.*, 2006; *McMurry et al.*, 2005], which are well above the upper limit of 100 ppt used in the THN parameterizations in this study. C_{NH3} of 100 ppt is thus used in calculating THN rates from NA02 and ME07 on both days.

[28] Figure 6 shows the simulated J values from various nucleation parameterizations with those observed during ANARChE on 31 July and 5 August 2002. Five parameterizations (i.e., FI98, KU98, VE02, YU06, and YU08) give J values below 1×10^{-8} cm^3 s^{-1}, which are not plotted. All calculated J values from NA02 are shown, although some may exceed the valid ranges of J values as specified by *Napari et al.* [2002]. The observed J values are in the range of 31–2784 and 0–436 cm^{-3} s^{-1}, respectively, on 31 July and 5 August 2002. WE94 and ME07 give zero J values for all 69 cases on 31 July and 47 cases on 5 August (thus not shown in the figures). VI02 also gives zero J values for more cases on 5 August and negligible values (<5.6 ×

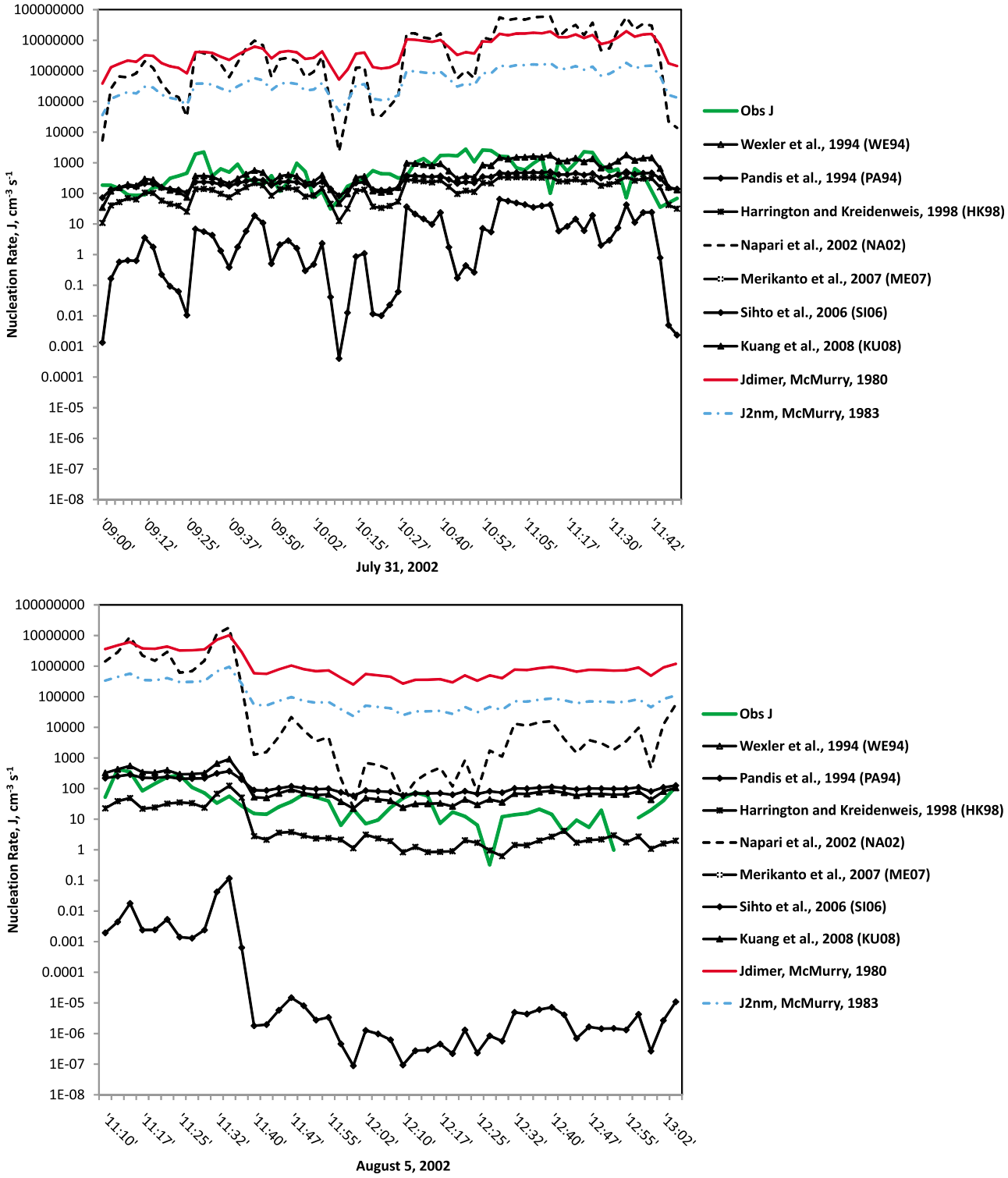

Figure 6. Simulated versus observed nucleation rates on (top) 31 July and (bottom) 5 August 2002. The observations are from *Kuang et al.* [2008] derived based on the Aerosol Nucleation and Real Time Characterization Experiment (ANARChE) study of nucleation during late July–August 2002. Five parameterizations (i.e., those of FI98, KU98, VE02, YU06, and YU08) give J values below 1×10^{-8} cm^3 s^{-1}, which are not plotted.

10^{-39} cm^{-3} s^{-1}) for the remaining cases on 5 August and all cases (<8.3×10^{-24} cm^{-3} s^{-1}) on 31 July, all of these nonzero values are well below its low valid limit of 1×10^{-7} cm^{-3} s^{-1} (results not shown). FI98, KU98, YU08, and YU06 give poor agreement with observations, with J values of 1.2×10^{-19}–8.8×10^{-11} cm^{-3} s^{-1}, 1.2×10^{-21}–$4.3 \times$

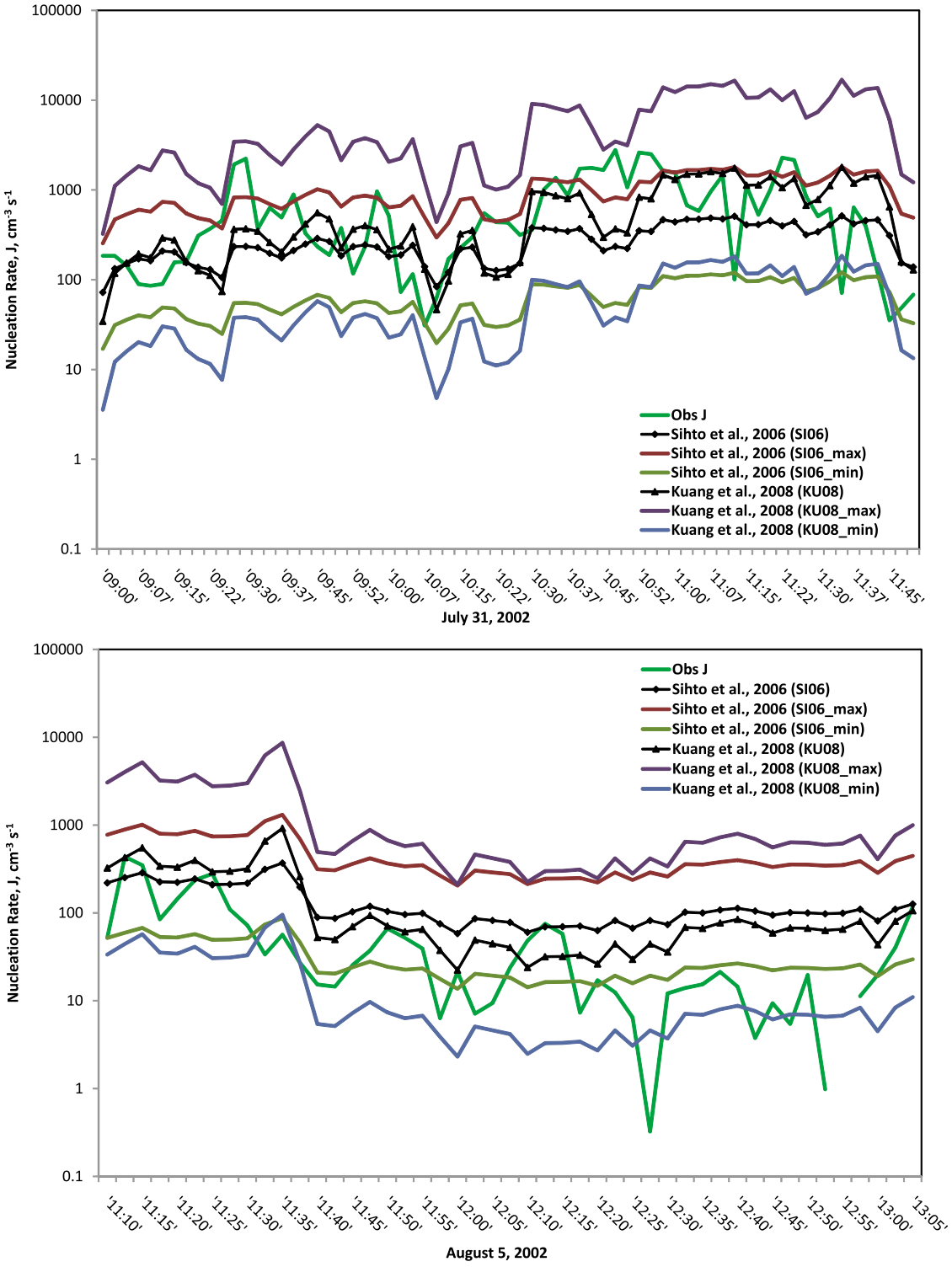

Figure 7. Simulated versus observed nucleation rates on (top) 31 July and (bottom) 5 August 2002 using work of *Sihto et al.* [2006] and *Kuang et al.* [2008]. SI06, SI06_min, and SI06_max refer to simulation results using the mean, minimal, and maximum prefactor A values of 1.7×10^{-6}, 6.0×10^{-6}, and 0.4×10^{-6}, respectively. Similarly, KU08, KU08_min, and KU08_max refer to simulation results using the minimal and maximum prefactor K values of 1.6×10^{-14}, 1.51×10^{-13}, and 1.66×10^{-15}, respectively.

10^{-14} cm^{-3} s^{-1}, 1.0×10^{-30}–9.4×10^{-16} cm^{-3} s^{-1}, 4.7×10^{-25}–1.8×10^{-11} cm^{-3} s^{-1}, respectively, and correlation coefficients of 0.08, 0.04, 0.17, and 0.16, respectively, on 31 July 2002 (results not shown). These parameterizations also give similar negligible J values and low correlation coefficients on 5 August. On the other hand, NA02 over-

Table 2. Performance Statistics for Various Nucleation Parameterizations Against Observations From ANARChE[a]

	0900–1150 LDT, 31 July 2002 Data Pair = 69, Mean Obs = 7.2E+02			1110–1305 LDT, 5 August 2002 Data Pair = 47, Mean Obs = 5.8E+01		
	Mean Sim	NMB, %	NME, %	Mean Sim	NMB, %	NME, %
Wexler et al. [1994] (WE94)	0.0E+00	−1.0E+02	1.0E+02	0.0E+00	−1.0E+02	1.0E+02
Pandis et al. [1994] (PA94)	1.0E+01	−9.9E+01	9.9E+01	4.2E-03	−1.0E+02	1.0E+02
Fitzgerald et al. [1998] (FI98)	5.4E-12	−1.0E+02	1.0E+02	6.5E-16	−1.0E+02	1.0E+02
Harrington and Kreidenweis [1998] (HK98)	1.6E+02	−7.8E+01	8.1E+01	1.3E+01	−7.8E+01	8.8E+01
Kulmala et al. [1998b] (KU98)[b]						
Vehkamäki et al. [2002] (VE98)[b]						
Yu [2008] (YU08)	5.7E-17	−1.0E+02	1.0E+02	8.1E-30	−1.0E+02	1.0E+02
Napari et al. [2002] (NA02)[c]	3.1E+05	4.4E+04	4.4E+04	4.5E+04	7.8E+04	7.8E+04
Merikanto et al. [2007b] (ME07)	0.0E+00	−1.0E+02	1.0E+02	0.0E+00	−1.0E+02	1.0E+02
Yu [2006b] (YU06)	1.4E-12	−1.0E+02	1.0E+02	1.0E-21	−1.0E+02	1.0E+02
Sihto et al. [2006] (SI06)	2.8E+02	−6.2E+01	7.3E+01	1.3E+02	1.3E+02	1.5E+02
Sihto et al. [2006] (SI06_min)[d]	6.5E+01	−9.1E+01	9.1E+01	3.1E+01	−4.7E+01	7.2E+01
Sihto et al. [2006] (SI06_max)[d]	9.7E+02	3.5E+01	8.2E+01	4.6E+02	6.9E+02	6.9E+02
Kuang et al. [2008] (KU08)	6.2E+02	−1.5E+01	7.2E+01	1.5E+02	1.6E+02	1.7E+02
Kuang et al. [2008] (KU08_min)[d]	6.4E+01	−9.1E+01	−9.1E+01	1.6E+01	−7.3E+01	−7.3E+01
Kuang et al. [2008] (KU08_max)[d]	5.8E+03	7.1E+02	7.1E+02	1.4E+03	2.3E+03	2.3E+03

[a]ANARChE, Aerosol Nucleation and Real Time Characterization Experiment; LDT, local daylight time; Mean Obs, mean observed value; Mean Sim, mean simulated value; NMB, normalized mean bias; and NME, normalized mean error.

[b]No entry indicates that the predicted J values are below the range of valid J values and no NMB and NME are calculated, which occurs for both KU98 and VE02.

[c]NA02 gives some rates that exceed the range of valid J (i.e., $>10^6$ cm^{-3} s^{-1}), which are excluded in the statistical calculation, resulting in fewer numbers of data pair for NA02 (i.e., 24 on 31 July and 38 on 5 August 2002) than other parameterizations (i.e., 69 on 31 July and 47 on 5 August 2002).

[d]SI06, SI06_min, and SI06_max refer to simulation results using the mean, minimal, and maximum prefactor A values of 1.7×10^{-6}, 6.0×10^{-6}, and 0.4×10^{-6}, respectively. Similarly, KU08, KU08_min, and KU08_max refer to simulation results using the minimal and maximum prefactor K values of 1.6×10^{-14}, 1.51×10^{-13}, and 1.66×10^{-15}, respectively.

predicts significantly, with J values of 2.3×10^3–6.1×10^7 cm^{-3} s^{-1} and a correlation coefficient of 0.2 on 31 July and 24.3–1.8×10^7 cm^{-3} s^{-1} and a correlation coefficient of 0.31 on 5 August (note that the valid range of J for NA02 is 10^{-5}–10^6 cm^{-3} s^{-1}). For comparison, PA94, HK98, SI06, KU08 perform better, with J rates of 4.0×10^{-4}–64 cm^{-3} s^{-1}, 11–354 cm^{-3} s^{-1}, 72–515 cm^{-3} s^{-1}, 35–1790 cm^{-3} s^{-1}, respectively, and correlation coefficients of 0.18, 0.35, 0.35, and 0.29, respectively, on 31 July and 8.9×10^{-8}–1.2×10^{-1} cm^{-3} s^{-1}, 6.2×10^{-1}–124 cm^{-3} s^{-1}, 58.2–370 cm^{-3} s^{-1}, 22.3–920 cm^{-3} s^{-1}, respectively, and correlation coefficients of 0.10, 0.42, 0.60, and 0.54, respectively, on 5 August.

[29] Four additional simulations using SI06 and KU08 are conducted to examine the sensitivity of simulated J values to the prefactors selected in SI06 and KU08: SI06_min and SI06_max using the minimal and maximum prefactor A values of 0.4×10^{-6} and 6.0×10^{-6}, respectively, and KU08_min and KU08_max using the minimal and maximum K values of 1.66×10^{-15} and 1.51×10^{-13}, respectively. Figure 7 shows the three sets of simulated J values for SI06 and KU08. Simulated J values vary by up to 2 orders of magnitudes on both days for SI06, and up to 4 and 3 orders of magnitudes on 31 July and 5 August, respectively, for KU08. For 31 July 2002, the J values using the max A for SI06 (i.e., SI06_max) and the mean prefactor K for KU08 (i.e., KU08) give the best fit among the respective three sets of results with SI06 and KU08, with KU08 giving the overall best agreement among all six simulations. For 5 August 2002, the J values using the min A for SI06 (i.e., SI06_min) and the min K for KU08 (i.e., KU08_min) give the best fit, with SI06_min giving the overall best agreement among all six simulations. These results illustrate the high sensitivity of the simulated J values to the prefactors used in the observation-fitted empirical power laws. Those power laws are derived from observations during certain time periods at specific locations, thus may not be applicable to locations that have very different atmospheric conditions.

[30] Table 2 summarizes the statistical performance of all parameterizations. The mean observed J is 719 cm^{-3} s^{-1} during 0900–1150 LDT on 31 July 2002. WE94 and ME07 give zero J values, FI98, KU98, VE02, YU08, and YU06 give negligible J values; those by KU98 and VE02 are smaller than their valid ranges of J values, thus no statistical calculation was performed for KU98 and VE02. The mean J values simulated by PA94, HK98, NA02, SI06, and KU08 are 10, 161, 3.1×10^5, 276, and 615 cm^{-3} s^{-1}, respectively. Note that only J values $\leq 1.0 \times 10^6$ cm^{-3} s^{-1} are used in the statistical calculation for NA02, because J values above this threshold are considered to be invalid [*Kulmala et al.*, 1998b]. The exclusion of invalid J values from NA02 results in only 24 valid data pairs out of a total of 69 data pairs for other parameterizations on 31 July. The mean J value based on the 24 data pairs for NA02 is lower than the corresponding mean J_{dimer} of 1.7×10^6 cm^{-3} s^{-1} but higher than mean $J_{2\ \text{nm}}$ of 1.6×10^5 cm^{-3} s^{-1}. Among the 12 parameterizations, KU08 gives the closest agreement with a normalized mean bias (NMB) of −14.6%, and SI06 and HK98 give the second and third closest agreement with NMBs of −61.7% and −77.7%, respectively. NA02 give the worst agreement with an NMB of $4.4 \times 10^{4\%}$. Using the min and max prefactors from SI06 and KU08 (i.e., SI06_min, SI06_max, KU08_min, and KU_max) will lead to greater underpredictions and overpredictions, respectively. During 1110–1305 LDT, 5 August 2002, the mean observed J is 58.06 cm^{-3} s^{-1}. WE94, FI98, KU98, VE02, YU06, YU08, and ME07 also give either zero or negligible

or invalid J values, the J values simulated by PA94, HK98, NA02, SI06, and KU08 are 4.2×10^{-3}, 12.7, 4.5×10^{4}, 131, and 151 cm^{-3} s^{-1}, respectively. The mean J value from NA02 is lower than mean J_{dimer} of 8.3×10^{5} cm^{-3} s^{-1} and J_{2nm} of 7.7×10^{4} cm^{-3} s^{-1} based on valid 38 data pairs on 5 August for NA02. Among the 12 parameterizations, HK98 gives the closest agreement with an NMB of −78.2%. Although SI06, and KU08 overpredict J values with NMBs of 125% and 160%, respectively, they perform much better than NA02, which gives the worst agreement with an NMB of 7.8×10^{4}%. Using the min prefactors from SI06 and KU08 (i.e., SI06_min and KU08_min) will improve their predictions in terms of NMB, whereas using the max prefactors from SI06 and KU08 (i.e., SI06_max and KU08_max) will lead to a greater overprediction since their simulated J values using the mean prefactors are already overpredicted. While these results illustrate the sensitivity of the simulated J values to the selected prefactors, no uniform prefactor can yield the best performance under all conditions. The mean prefactors are therefore used by SI06 and KU08 in the 3-D model evaluation in part 2 [*Zhang et al.*, 2010].

6. Conclusions

[31] A total of 12 nucleation parameterizations that are based on various nucleation theories are evaluated under a variety of atmospheric conditions from surface to mesosphere. Significant differences are found among the nucleation rates calculated with different binary, ternary, and power law parameterizations under the same T, RH, and N_{H2SO4} conditions (e.g., by up to 15 orders of magnitude under conditions with T = 258.15 K, RH = 50%, and $N_{H2SO4} = 2 \times 10^{7}$ cm^{-3} or up to 18 orders of magnitude under conditions with T = 298.15 K, RH = 80%, and $N_{H2SO4} = 8 \times 10^{9}$ cm^{-3}). These parameterizations generally give a strong linear or nonlinear dependence of $\log(J)$ on $\log(N_{H2SO4})$ that consistently gives higher J values under higher N_{H2SO4} levels. All except for WE94, PA94, SI06, and KU08 show a strong T dependence, with J values decrease with increasing T for most parameterizations except for HK98, which gives higher J values at higher T for $T < 240$ K under all N_{H2SO4} levels, and KU98, which gives higher J values when T increases for $T <$ 240 K under conditions with a high N_{H2SO4} of 10^{9} cm^{-3}. All except for SI06 and KU08 show an RH dependence, with J values increase with increasing RH for most parameterizations except for NA02 and ME07, which gives lower J values when RHs increase, and FI98, which gives J values decreasing with increased RHs from 0 to 30% but J values increasing with increased RHs when RH further increases to 100%. Among the THN parameterizations, both NA02 and ME07 show a strong dependence on NH_3, with J values from NA02 higher by up to 11 orders of magnitude than those from ME07 and YU06 under the middle tropospheric and urban surface conditions. The differences in J values in terms of magnitude and dependence on influential parameters such as N_{H2SO4}, T, RH, and C_{NH3} are attributed to different theories/models based, other processes (e.g., condensation) considered, mathematical formulations used, and in a few cases, the technical flaws and assumptions associated with the derivation of some parameterizations (e.g., KU98 and NA02).

[32] Compared with J_{dimer} and J_{2nm}, some J values exceed these upper limits, including all rates by NA02 at $C_{NH3} >$ 0.1 ppt, nearly all rates by WE94, and some rates by PA94, FI98, VE02, and NA02 at C_{NH3} = 0.1 ppt at some N_{H2SO4} in the range of 10^{4}–10^{12} cm^{-3} under the middle tropospheric and/or urban surface conditions. Several parameterizations give rates much higher than J_{dimer} and $J_{2\ nm}$ including those of FI98 at $T < 240$ K and NA02 at $T > 240$ K at some T values under the conditions with RH = 50% and $N_{H2SO4} = 10^{4}$ cm^{-3} and WE94 at all T values, FI98 at $T < 290$ K, and VI02 at $T < 250$ K under the conditions with RH = 80% and $N_{H2SO4} = 10^{9}$ cm^{-3}. The J rates simulated by NA02 at C_{NH3} = 100 ppt for all RH values under the conditions with T = 258.15 K and $N_{H2SO4} = 10^{4}$ cm^{-3} and those by WE94 at $RH > 0.6$, PA94 at $RH >$ 50%, and FI98 at $RH > 0.95$ under the conditions with T = 298.15 K and $N_{H2SO4} = 10^{9}$ cm^{-3} exceed J_{dimer} and $J_{2\ nm}$. SI06 at all RHs gives a rate that is slightly lower than J_{dimer} but higher than $J_{2\ nm}$. KU08 gives a constant rate of 1.8×10^{-6} cm^{-3} s^{-1}, which is well below J_{dimer} and $J_{2\ nm}$. NA02 gives rates that are higher than J_{dimer} or $J_{2\ nm}$, respectively, at some or all C_{NH3} values under the middle tropospheric condition with RH = 50%, T = 258.15 K, and $N_{H2SO4} > 10^{4}$ cm^{-3} and at some C_{NH3} values under the urban surface conditions with RH = 80%, T = 298.15 K, and N_{H2SO4} of 10^{9} cm^{-3}. WE94 and PA94 also give rates above J_{dimer} or $J_{2\ nm}$ for all ranges of C_{NH3} under the same urban surface conditions. Among all parameterizations, only KU98, YU06, YU08, ME07, and KU08 do not give rates that are higher than either J_{dimer} or $J_{2\ nm}$ under atmospheric conditions considered in this study. HK98 does not exceed those limits under most conditions and SI06 does not exceed J_{dimer} but does exceed $J_{2\ nm}$ under some conditions. The remaining parameterizations often exceed those limits under many atmospheric conditions tested. These parameterizations should therefore be used with caution under the above conditions in 3-D air quality models. Their rates should be capped at a reasonable value such as J_{dimer} if such a growth is not accounted for and a minimal measureable detectable particle size is assumed to calculate the new particle formation rates based on the nucleation rates simulated by these parameterizations.

[33] Under the laboratory experimental conditions, calculated J by various parameterizations can vary orders of magnitude from measurements. When comparing with measured J of *Ball et al.* [1999] that used the liquid samples of H_2SO_4, YU08 and HK98 give the closest agreement with measured BHN rates and YU06 gives the closest agreement with measured THN rates at T = 295 K and RH = 4.6%, and KU98 and YU06 give the closest agreement with measured BHN and THN rates, respectively, at T = 295 K and RH = 15.3%. The enhancement in J values calculated by NA02 relative to KU98 and VE02 based on classical nucleation theories is up to several tenths orders of magnitude higher than those observed in the laboratory (on the order of 1–3). The power laws of SI06 and KU08 give J values that are higher by up to 6–8 orders of magnitude than measured BHN and THN rates under low-RH conditions. When comparing with measured J with H_2SO_4 generated from the SO_2 + OH reactions [e.g., *Berndt et al.*, 2005, 2006, 2010; *Benson et al.*, 2009], SI06 and KU08 give the best overall agreement.

[34] Compared with observed J rates at JST from ANARChE during summer 2002, WE94 and ME07 give zero J values, KU98 and VE02 give invalid J values, and FI98, YU08, and YU06 give negligible J values on both 31 July and 5 August, the J values simulated by NA02 are much higher than observations with an NMB of 4.3–7.8 $\times$ $10^{4\%}$, those from PA94, HK98, SI06, and KU08 are more reasonable, with NMBs of −77.7% to 160%, despite large negative or positive biases. Overall, KU08, HK98, and SI06 give the best agreement among the 12 parameterizations tested under the sulfate-rich urban environment in the southeastern United States.

[35] One limitation of this study is that this work focuses on nucleation in the ambient atmosphere and may not be applicable to nucleation under other conditions (e.g., nucleation of particles in vehicle exhausts under high-T conditions). Another limitation is that the parameterization evaluation results are obtained in a box model that neglects the impact of other atmospheric processes including transport, emission, dry and wet removal, as well as other aerosol processes such as condensation, coagulation, and dissolution on J and its dependent variables. Examining the combined effect of these processes for an accurate simulation of atmospheric aerosol formation and evolution requires the use of a 3-D air quality model, and is the main focus of part 2 [*Zhang et al.*, 2010].

[36] Among all parameterizations, KU08 does not exceed the upper limit nucleation and new particle formation rates and gives an overall good agreement with the observed J rates under the sulfate-rich urban environment in Atlanta, providing the most plausible nucleation parameterization under such conditions. HK98 and SI06 also give reasonably good results despite occasional exceedances of the upper limit rates, which can be overcome through capping their rates with those upper limits in 3-D simulations. It should be pointed out that KU08 and SI06 do not depend on T and RH, and the prefactors in these empirical activation or kinetic formulas derived from different field measurements may vary by up to 4 orders of magnitude [*Kuang et al.*, 2008]. It remains to be studied what controls the values of these prefactors. Recent global modeling studies indicate that the empirical activation and kinetic formulas significantly overpredict new particle formation in the warm tropical regions [*Yu et al.*, 2010]. In addition, those empirical power laws give much higher nucleation rates than some laboratory measurements [e.g., *Ball et al.*, 1999] due likely to the fact that they were derived under very different ambient atmospheric conditions (e.g., much higher RH conditions than the laboratory conditions); the consideration of T and RH dependence in such empirical expressions may be necessary to improve their prediction skills under such conditions.

[37] Although KU98, YU06, YU08, and ME07 do not exceed the upper limit nucleation and new particle formation rates, their J values, however, are too low to represent the observed J rates. In particular, ME07 does not predict nucleation under most atmospheric conditions and KU98 has technical mistakes. These parameterizations are therefore not recommended for applications under the urban environment, although they may work well under other atmospheric conditions (e.g., upper troposphere/stratosphere or less polluted boundary layers). The remaining nucleation parameterizations give rates that often exceed the upper limit rates and also do not give a good agreement with observed J rates under the urban polluted conditions, their applications in 3-D models should be given extra cautions and the upper limit rates should always be used to cap their simulated J rates. Among those highly uncertain or problematic parameterizations, WE94 and NA02 are not recommended for 3-D applications for very clean to highly polluted atmospheres. The nucleation rates from WE94 exceed the upper limits under most atmospheric conditions. Those from NA02 also exceed the upper limits under many conditions. In addition, NA02 has several fundamental problems associated with their formulation. As a result, the ternary rates from NA02 at C_{NH3} = 100 ppt are higher by 4–15 orders of magnitude than rates by most BHN parameterizations, two power laws, and other THN parameterizations (e.g., YU06 and ME07). These results are consistent with findings from several studies [e.g., *Anttila et al.*, 2005; *Lucas and Akimoto*, 2006; *Yu*, 2006b; *Merikanto et al.*, 2007b] that reported unrealistically high nucleation rates from NA02. Such high nucleation rates are not supported by laboratory studies and field observations in the planetary boundary layer [e.g., *Kim et al.*, 1998; *Ball et al.*, 1999]. In addition, the nucleation rates simulated by NA02 are inconsistent with observed enhancement factors for nucleation rates with C_{NH3} of several ppt to several ppm. The RH dependence of nucleation rates of NA02 is also inconsistent with laboratory observations and other nucleation parameterizations. Although some studies show that NA02 gives a good agreement with particle observations under rural and urban conditions [e.g., *Jung et al.*, 2008, 2010; *Elleman and Covert*, 2009b], it is questionable whether the good agreement was obtained for right reasons. KU98 and the updated version of VE02 give rates that are too low to match with observed J rates in the laboratory and during the summer 2002 ANARChE field campaign under surface ambient conditions, and VE02 sometimes gives rates that are above the upper limit rates under low-temperature conditions (e.g., under conditions with N_{H2SO4} = 1×10^5 cm^{-3}, RH = 50%, and T < 210 K, and with N_{H2SO4} = 1×10^9 cm^{-3}, RH = 80% and T < 250 K, as shown in Figure 2), they are therefore also not recommended for applications for polluted boundary layer.

[38] As demonstrated in this study, simulating nucleation under ambient atmospheric conditions and in vehicle exhaust is a difficult task with substantial uncertainties. Major challenges include (1) the nucleation mechanism and the participating chemical species are often unknown; (2) small changes in free energy can affect the nucleation rate exponentially [*Jacobson*, 2005]; (3) difficulties in accurately calculating saturation ratio and its continuous changes, resulting in nucleation rates several orders of magnitude off [*Brus et al.*, 2009]; (4) calculation of nucleation rates is computationally demanding due to the complexity in dealing with the detailed nucleation kinetics and thermodynamics [e.g., *Arstila et al.*, 1999; *Lazaridis*, 2001]; (5) the classical theory is based on a concept of a liquid droplet on a macroscopic scale that is not applicable to smaller molecular-scale clusters [*Oxtoby*, 1998; *Kulmala*, 2003; *Seinfeld and Pandis*, 2006]; (6) various parameterizations, derived from either empirical approaches or classical nucleation theories, predict nucleation rates that differ by many orders of magnitude; (7) most nucleation parameterizations are

developed for atmospheric conditions and it is not clear whether they are applicable to nucleation at the high temperatures associated with engine exhausts; and (8) various approaches used to represent particle size distribution (e.g., modal versus sectional [*Zhang et al.*, 1999; *Korhonen et al.*, 2003; *Pirjola et al.*, 2004]) as well as the growth of cluster into minimal measurable particle sizes [e.g., *Kerminen and Kulmala*, 2002; *Elleman and Covert*, 2009b] may also introduce additional uncertainties. In addition to challenges with calculating nucleation rates, atmospheric models must also correctly calculate growth rates. Measured growth rates are typically about 10 times higher than those that can be explained by H_2SO_4 condensation alone [*Kulmala et al.*, 2001a; *Stolzenburg et al.*, 2005], which may be explained by condensation of organic compounds [e.g., *Q. Zhang et al.*, 2004; *McMurry et al.*, 2005]. Recent work has also shown that the uptake of aminium salts by freshly nucleated particles helps explain these high growth rates [*Smith et al.*, 2010], although the mechanism by which these salts are taken up is not yet understood.

[39] **Acknowledgments.** This work was supported by the NSF award Atm-0348819, the NOAA award NA03NES4400015, the Memorandum of Understanding between the U.S. Environmental Protection Agency (EPA) and the U.S. Department of Commerce's National Oceanic and Atmospheric Administration (NOAA) under agreement DW13921548, and the National Research Initiative competitive grant 2008-35112-18758 from the USDA Cooperative State Research, Education, and Extension Service Air Quality Program at North Carolina State University. P.H.M. acknowledges support from NSF award ATM-050067. F.Y. acknowledges support from NSF award AGS-0942106. Thanks are owed to Hanna Vehkamäki, University of Helsinki, Finland, for providing a corrected version of code for *Merikanto et al.* [2007b] parameterization; Chongai Kuang, Brookhaven National Laboratory, for providing observed H_2SO_4, RH, and T, and derived nucleation rates based on particle size measurements from ANARChE; L. Greg Huey, Georgia Institute of Technology, for providing NH_3 measurement data from ANARChE; and T. Berndt and M. Sipila, Leibniz-Institut Für Troposphärenforschung e.V., and S.-H. Lee, Kent State University, for providing their laboratory nucleation measurements for the evaluation of various nucleation parameterizations. Thanks are also owed to Prakash V. Bhave, U.S. EPA, for helpful review and discussions.

References

Anttila, T., H. Vehkamäki, I. Napari, and M. Kulmala (2005), Effect of ammonium bisulphate formation on atmospheric water-sulphuric acid-ammonia nucleation, *Boreal Environ. Res.*, *10*, 511–523.

Arstila, H., P. Korhonen, and M. Kulmala (1999), Ternary nucleation: Kinetics and application to water-ammonia-hydrochloric acid system, *J. Aerosol Sci.*, *30*, 131–138, doi:10.1016/S0021-8502(98)00033-0.

Ball, S. M., D. R. Hanson, F. L. Eisele, and P. H. McMurry (1999), Laboratory studies of particle nucleation: Initial results for H_2SO_4, H_2O, and NH_3 vapors, *J. Geophys. Res.*, *104*, 23,709–23,718, doi:10.1029/1999JD900411.

Benson, D. R., M. E. Erupe, and S.-H. Lee (2009), Laboratory-measured H_2SO_4-H_2O-NH_3 ternary homogeneous nucleation rates: Initial observations, *Geophys. Res. Lett.*, *36*, L15818, doi:10.1029/2009GL038728.

Berndt, T., O. Boge, F. Stratmann, J. Heintzenberg, and M. Kulmala (2005), Rapid formation of sulfuric acid particles at near-atmospheric conditions, *Science*, *307*, 698–700, doi:10.1126/science.1104054.

Berndt, T., O. Boge, and F. Stratmann (2006), Formation of atmospheric H_2SO_4-H_2O particles in the absence of organics: A laboratory study, *Geophys. Res. Lett.*, *33*, L15817, doi:10.1029/2006GL026660.

Berndt, T., F. Stratmann, S. Brasel, J. Heintzenberg, A. Laaksonen, and M. Kulmala (2008), SO_2 oxidation products other than H_2SO_4 as a trigger of new particle formation—Part 1: Laboratory investigations, *Atmos. Chem. Phys.*, *8*, 6365–6374, doi:10.5194/acp-8-6365-2008.

Berndt, T., et al. (2010), Laboratory study on new particle formation from the reaction OH + SO_2: Influence of experimental conditions, H_2O vapour, NH_3 and the amine tert-butylamine on the overall process, *Atmos. Chem. Phys. Discuss.*, *10*, 6447–6484, doi:10.5194/acpd-10-6447-2010.

Binkowski, F. S., and S. J. Roselle (2003), Models-3 community multiscale air quality (CMAQ) model aerosol component: 1. Model description, *J. Geophys. Res.*, *108*(D6), 4183, doi:10.1029/2001JD001409.

Birmili, W., and A. Wiedensohler (1998), The influence of meteorological parameters on ultrafine particle production at a continental site, *J. Aerosol Sci.*, *29*, S1015–S1016, doi:10.1016/S0021-8502(98)90690-5.

Boy, M., et al. (2005), Sulphuric acid closure and contribution to nucleation mode particle growth, *Atmos. Chem. Phys.*, *5*, 863–878, doi:10.5194/acp-5-863-2005.

Brock, C. A., et al. (2003), Particle growth in the plumes of coal-fired power plan, *J. Geophys. Res.*, *108*(D3), 4111, doi:10.1029/2002JD002746.

Brus, D., V. Ždímal, and H. Uchtmann (2009), Homogeneous nucleation rate measurements in supersaturated water vapor II, *J. Chem. Phys.*, *131*, 074507, doi:10.1063/1.3211105.

Byun, D., and K. L. Schere (2006), Review of the governing equations, computational algorithms, and other components of the Models-3 Community Multiscale Air Quality (CMAQ) modeling system, *Appl. Mech. Rev.*, *59*, 51–77, doi:10.1115/1.2128636.

Clarke, A. D. (1992), Atmospheric nuclei in the remote free troposphere, *J. Atmos. Chem.*, *14*, 479–488, doi:10.1007/BF00115252.

Clarke, A. D., J. L. Varner, F. Eisele, R. L. Mauldin, D. Tanner, and M. Litchy (1998), Particle production in the remote marine atmosphere: Cloud outflow and subsidence during ACE 1, *J. Geophys. Res.*, *103*, 16,397–16,409, doi:10.1029/97JD02987.

Coffman, D. J., and D. A. Hegg (1995), A preliminary study of the effect of ammonia on particle nucleation in the marine boundary layer, *J. Geophys. Res.*, *100*, 7147–7160, doi:10.1029/94JD03253.

Covert, D. S., V. N. Kapustin, P. K. Quinn, and T. S. Bates (1992), New particle formation in the marine boundary layer, *J. Geophys. Res.*, *97*, 20,581–20,589.

Eisele, F. L., E. R. Lovejoy, E. Kosciuch, K. F. Moore, R. L. Mauldin III, J. N. Smith, P. H. McMurry, and K. Iida (2006), Negative atmospheric ions and their potential role in ion-induced nucleation, *J. Geophys. Res.*, *111*, D04305, doi:10.1029/2005JD006568.

Elleman, R. A., and D. S. Covert (2009a), Aerosol size distribution modeling with the Community Multiscale Air Quality modeling system in the Pacific Northwest: 1. Model comparison to observations, *J. Geophys. Res.*, *114*, D11206, doi:10.1029/2008JD010791.

Elleman, R. A., and D. S. Covert (2009b), Aerosol size distribution modeling with the Community Multiscale Air Quality modeling system in the Pacific Northwest: 2. Parameterizations for ternary nucleation and nucleation mode processes, *J. Geophys. Res.*, *114*, D11207, doi:10.1029/2009JD012187.

Fitzgerald, J. W., W. A. Hoppel, and F. Gelbard (1998), A one-dimensional sectional model to simulate multicomponent aerosol dynamics in the marine boundary layer: 1. Modal description, *J. Geophys. Res.*, *103*, 16,085–16,102, doi:10.1029/98JD01019.

Griffin, R. J., D. Dabdub, M. J. Kleeman, M. P. Fraser, G. R. Cass, and J. H. Seinfeld (2002), Secondary organic aerosol: III. Urban/regional scale model of size- and composition-resolved aerosols, *J. Geophys. Res.*, *107*(D17), 4334, doi:10.1029/2001JD000544.

Harrington, D. Y., and S. M. Kreidenweis (1998), Simulation of sulfate aerosol dynamics. I. Model description, *Atmos. Environ.*, *32*, 1691–1700, doi:10.1016/S1352-2310(97)00452-4.

Hoffmann, T., C. D. O'Dowd, and J. H. Seinfeld (2001), Iodine oxide homogeneous nucleation: An explanation for coastal new particle production, *Geophys. Res. Lett.*, *28*(10), 1949–1952.

Ianni, J. C., and A. R. Bandy (1999), A density functional theory study of the hydrates of $NH_3 \cdot H_2SO_4$ and its implications for the formation of new atmospheric particles, *J. Phys. Chem. A*, *103*, 2801, doi:10.1021/jp983608r.

Jacobson, M. Z. (1997), Development and application of a new air pollution modeling system–II. Aerosol module structure and design, *Atmos. Environ.*, *31*, 131–144, doi:10.1016/1352-2310(96)00202-6.

Jacobson, M. Z. (2001), GATOR-GCMM, A global through urban scale air pollution and weather forecast model: 1. Model design and treatment of subgrid soil, vegetation, roads, rooftops, water, sea ice, and snow, *J. Geophys. Res.*, *106*, 5385–5401, doi:10.1029/2000JD900560.

Jacobson, M. Z. (2004), The climate response of fossil-fuel and biofuel soot, accounting for soot's feedback to snow and sea ice albedo and emissivity, *J. Geophys. Res.*, *109*, D21201, doi:10.1029/2004JD004945.

Jacobson, M. Z. (2005), *Fundamentals of Atmospheric Modeling*, 2nd ed., Cambridge Univ. Press, Cambridge, U. K.

Jaecker-Voirol, A., and P. Mirabel (1989), Heteromolecular nucleation in the sulfuric acid-water system, *Atmos. Environ.*, *23*, 2033–2057.

Jung, J. G., S. N. Pandis, and P. J. Adams (2008), Evaluation of nucleation theories in a sulfur-rich environment, *Aerosol Sci. Technol.*, *42*, 495–504, doi:10.1080/02786820802187085.

Jung, J., C. Fountoukis, P. J. Adams, and S. N. Pandis (2010), Simulation of in situ ultrafine particle formation in the eastern United States using PMCAMx-UF, *J. Geophys. Res.*, *115*, D03203, doi:10.1029/2009JD012313.

Kerminen, V.-M., and M. Kulmala (2002), Analytical formulae connecting the "real" and the "apparent" nucleation rate and the nuclei number concentration for atmospheric nucleation events, *J. Aerosol Sci.*, *33*, 609–622, doi:10.1016/S0021-8502(01)00194-X.

Kim, T. O., T. Ishida, M. Adachi, K. Okuyama, and J. H. Seinfeld (1998), Nanometer-sized particle formation from $NH_3/SO_2/H_2O$/air mixtures by ionizing irradiation, *Aerosol Sci. Technol.*, *29*, 111–125, doi:10.1080/02786829808965556.

Korhonen, H., K. E. J. Lehtinen, L. Pirjola, I. Napari, H. Vehkamäki, M. Noppel, and M. Kulmala (2003), Simulation of atmospheric nucleation mode: A comparison of nucleation models and size distribution representations, *J. Geophys. Res.*, *108*(D15), 4471, doi:10.1029/2002JD003305.

Korhonen, P., M. Kulmala, A. Laaksonen, Y. Viisanen, R. McGraw, and J. H. Seinfeld (1999), Ternary nucleation of H_2SO_4, NH_3, H_2O in the atmosphere, *J. Geophys. Res.*, *104*, 26,349–26,353, doi:10.1029/1999JD900784.

Kuang, C., P. H. McMurry, A. V. McCormick, and F. L. Eisele (2008), Dependence of nucleation rates on sulfuric acid vapor concentration in diverse atmospheric locations, *J. Geophys. Res.*, *113*, D10209, doi:10.1029/2007JD009253.

Kuang, C., P. H. McMurry, and A. V. McCormick (2009), Determination of cloud condensation nuclei production from measured new particle formation events, *Geophys. Res. Lett.*, *36*, L09822, doi:10.1029/2009GL037584.

Kulmala, M. (2003), How particles nucleate and grow, *Science*, *302*, 1000–1001, doi:10.1126/science.1090848.

Kulmala, M., A. Toivonen, J. M. Makela, and A. Laaksonen (1998a), Analysis of the growth of nucleation mode particles observed in Boreal forest, *Tellus, Ser. B*, *50*, 449–462, doi:10.1034/j.1600-0889.1998.t01-4-00004.x.

Kulmala, M., A. Laaksonen, and L. Pirjola (1998b), Parameterizations for sulphric acid/water nucleation rates, *J. Geophys. Res.*, *103*, 8301–8307, doi:10.1029/97JD03718.

Kulmala, M., L. Pirjola, and J. M. Mäkelä (2000), Stable sulphate clusters as a source of new atmospheric particles, *Nature*, *404*, 66–69, doi:10.1038/35003550.

Kulmala, M., M. Dal Maso, J. Mäkelä, L. Pirjola, M. Väkevä, P. Aalto, P. Mikkulainen, K. Hämeri, and C. O'Dowd (2001a), On the formation, growth and composition of nucleation mode particles, *Tellus, Ser. B*, *53*, 479–490, doi:10.1034/j.1600-0889.2001.d01-33.x.

Kulmala, M., et al. (2001b), Overview of the international project on Biogenic aerosol formation in the boreal forest (BIOFOR), *Tellus, Ser. B*, *53*, 324–343.

Kulmala, M., K. Lehtinen, and A. Laaksonen (2006), Cluster activation theory as an explanation of the linear dependence between formation rate of 3 nm particles and sulphuric acid concentration, *Atmos. Chem. Phys.*, *6*, 787–793, doi:10.5194/acp-6-787-2006.

Kurtén, T., L. Torpo, C.-G. Ding, H. Vehkamäki, M. R. Sundberg, K. Laasonen, and M. Kulmala (2007), A density functional study on water-sulfuric acid ammonia clusters and implications for atmospheric cluster formation, *J. Geophys. Res.*, *112*, D04210, doi:10.1029/2006JD007391.

Kurtén, T., V. Loukonen, H. Vehkamaki, and M. Kulmala (2008), Amines are likely to enhance neutral and ion-induced sulfuric acid-water nucleation in the atmosphere more effectively than ammonia, *Atmos. Chem. Phys.*, *8*, 4095–4103, doi:10.5194/acp-8-4095-2008.

Laakso, L., et al. (2004), Kinetic nucleation and ions in boreal forest particle formation events, *Atmos. Chem. Phys.*, *4*, 2353–2366, doi:10.5194/acp-4-2353-2004.

Laaksonen, A., A. Hamde, J. Joutsensaari, L. Hiltunen, F. Cavalli, W. Junkermann, A. Asmi, S. Fuzzi, and M. C. Faccini (2005), Cloud condensation nucleus production from nucleation events at a highly polluted region, *Geophys. Res. Lett.*, *32*, L06812, doi:10.1029/2004GL022092.

Lazaridis, M. (2001), New particle formation of ternary droplets in the atmosphere a steady-state nucleation kinetics approach, *Atmos. Environ.*, *35*, 599–607, doi:10.1016/S1352-2310(00)00293-4.

Lee, S. H., J. M. Reeves, J. C. Wilson, D. E. Hunton, A. A. Viggiano, T. M. Miller, J. O. Ballenthin, and L. R. Lait (2003), Particle formation by ion nucleation in the upper troposphere and lower stratosphere, *Science*, *301*, 1886–1889, doi:10.1126/science.1087236.

Lovejoy, E. R., J. Curtius, and K. D. Froyd (2004), Atmospheric ion-induced nucleation of sulfuric acid and water, *J. Geophys. Res.*, *109*, D08204, doi:10.1029/2003JD004460.

Lucas, D. D., and H. Akimoto (2006), Evaluating aerosol nucleation parameterizations in a global atmospheric model, *Geophys. Res. Lett.*, *33*, L10808, doi:10.1029/2006GL025672.

Lushnikov, A. A., and M. Kulmala (1998), Dimers in nucleating vapors, *Phys. Rev. E*, *58*(3), 3157–3167, doi:10.1103/PhysRevE.58.3157.

Mäkelä, J. M., P. Aalto, V. Jokinen, A. Nissinen, S. Palmroth, T. Markkanen, K. Seitsonen, H. Lihavainen, and M. Kulmala (1997), Observations of ultrafine aerosol particle formation and growth in boreal forest, *Geophys. Res. Lett.*, *24*(10), 1219–1222, doi:10.1029/97GL00920.

Marti, J. J., R. J. Weber, and P. H. McMurry (1997), new particle formation at a remote continental site: Assessing the contributions of SO_2 and organic precursors, *J. Geophys. Res.*, *102*, 6331–6339, doi:10.1029/96JD02545.

McFiggans, G., J. M. C. Plane, B. J. Allan, L. J. Carpenter, H. Coe, and C. D. O'Dowd (2000), A modeling study of iodine chemistry in the marine boundary layer, *J. Geophys. Res.*, *105*, 14,371–14,385, doi:10.1029/1999JD901187.

McGovern, F. M. (1999), An analysis of condensation nuclei levels at Mace Head, Ireland, *Atmos. Environ.*, *33*, 1711–1723, doi:10.1016/S1352-2310(98)00242-8.

McMurry, P. H. (1980), Photochemical aerosol formation from SO_2: A theoretical analysis of smog chamber data, *J. Colloid Interface Sci.*, *78*, 513–527, doi:10.1016/0021-9797(80)90589-5.

McMurry, P. H. (1983), New particle formation in the presence of an aerosol: rates, time scales, and sub-0.01 μm size distributions, *J. Colloid Interface Sci.*, *95*, 72–80, doi:10.1016/0021-9797(83)90073-5.

McMurry, P., and F. Eisele (2005), Preface to topical collection on new particle formation in Atlanta, *J. Geophys. Res.*, *110*, D22S01, doi:10.1029/2005JD006644.

McMurry, P. H., and S. K. Friedlander (1979), New particle formation in the presence of an aerosol, *Atmos. Environ.*, *13*, 1635–1651, doi:10.1016/0004-6981(79)90322-6.

McMurry, P. H., K. S. Woo, R. Weber, D.-R. Chen, and D. Y. H. Pui (2000), Size distributions of 3–10 nm atmospheric particles: Implications for nucleation mechanisms, *Philos. Trans. R. Soc., Ser. A*, *358*, 2625–2642, doi:10.1098/rsta.2000.0673.

McMurry, P., M. Fink, H. Sakurai, M. Stolzenburg, L. Mauldin, K. Moore, J. Smith, F. Eisele, S. Sjostedt, and D. Tanner (2005), A criterion for new particle formation in the sulfur-rich Atlanta atmosphere, *J. Geophys. Res.*, *110*, D22S02, doi:10.1029/2005JD005901.

McMurry, P. H., C. Kuang, J. N. Smith, J. Zhao, and F. Eisele (2010), Atmospheric new particle formation: Physical and chemical measurements, in *Aerosol Measurement—Principles, Techniques, and Applications*, 3rd ed., edited by P. Kulkarni, P. A. Baron, and K. Willeke, chap. 31 pp., John Wiley, Hoboken, N. J., in press.

Merikanto, J., E. Zapadinsky, A. Lauri, and H. Vehkamäki (2007a), Origin of the failure of classical nucleation theory: Incorrect description of the smallest clusters, *Phys. Rev. Lett.*, *98*, 145702, doi:10.1103/PhysRevLett.98.145702.

Merikanto, J., I. Napari, H. Vehkamäki, T. Anttila, and M. Kulmala (2007b), New parameterization of sulfuric acid-ammonia-water ternary nucleation rates at tropospheric conditions, *J. Geophys. Res.*, *112*, D15207, doi:10.1029/2006JD007977.

Merikanto, J., D. V. Spracklen, G. W. Mann, S. J. Pickering, and K. S. Carslaw (2009a), Impact of nucleation on global CCN, *Atmos. Chem. Phys.*, *9*, 8601–8616, doi:10.5194/acp-9-8601-2009.

Merikanto, J., I. Napari, H. Vehkamäki, T. Anttila, and M. Kulmala (2009b), Correction to "New parameterization of sulfuric acid–ammonia-water ternary nucleation rates at tropospheric conditions", *J. Geophys. Res.*, *114*, D09206, doi:10.1029/2009JD012136.

Nadykto, A. B., and F. Yu (2007), Strong hydrogen bonding between atmospheric nucleation precursors and organic acids, *Chem. Phys. Lett.*, *435*, 14–18, doi:10.1016/j.cplett.2006.12.050.

Nadykto, A. B., F. Yu, and J. Herb (2009), Ammonia in positively charged atmospheric pre-nucleation clusters: A quantum-chemical study and atmospheric implications, *Atmos. Chem. Phys.*, *9*, 4031–4038, doi:10.5194/acp-9-4031-2009.

Napari, I., M. Noppel, H. Vehkamäki, and M. Kulmala (2002), Parameterization of ternary nucleation rates for H_2SO_4-NH_3-H_2O vapors, *J. Geophys. Res.*, *107*(D19), 4381, doi:10.1029/2002JD002132.

Noppel, M., H. Vehkamäki, and M. Kulmala (2002), An improved model for hydrate formation in sulfuric acid-water nucleation, *J. Chem. Phys.*, *116*, 218–228, doi:10.1063/1.1423333.

Nowak, J., et al. (2006), Analysis of urban gas-phase ammonia measurements from the 2002 Atlanta Aerosol Nucleation and Real-time Characterization Experiment (ANARChE), *J. Geophys. Res.*, *111*, D17308, doi:10.1029/2006JD007113.

O'Dowd, C. D., and T. Hoffmann (2005), Coastal new particle formation: A review of the current state of the art, *Environ. Chem.*, *2*, 245–255, doi:10.1071/EN05077.

O'Dowd, C. D., et al. (1999), On the photochemical production of new particles in the coastal boundary layer, *Geophys. Res. Lett.*, *26*(12), 1707–1710, doi:10.1029/1999GL900335.

O'Dowd, C. D., J. L. Jimenez, R. Bahreini, R. C. Flagan, J. H. Seinfeld, K. Hämeri, L. Pirjola, M. Kulmala, S. G. Jennings, and T. Hoffmann (2002), Marine aerosol formation from biogenic iodine emissions, *Nature*, *417*, 632–636, doi:10.1038/nature00775.

Oxtoby, D. W. (1998), Nucleation of first-order phase transitions, *Acc. Chem. Res.*, *31*, 91–97, doi:10.1021/ar9702278.

Pandis, S. N., L. M. Russell, and J. H. Seinfeld (1994), The relationship between DMS flux and CCN concentration in remote marine regions, *J. Geophys. Res.*, *99*, 16,945–16,957, doi:10.1029/94JD01119.

Pierce, J. R., and P. J. Adams (2009), Uncertainty in global CCN concentrations from uncertain aerosol nucleation and primary emission rate, *Atmos. Chem. Phys.*, *9*, 1339–1356, doi:10.5194/acp-9-1339-2009.

Pirjola, L., K. E. J. Lehtinen, H.-C. Hansson, and M. Kulmala (2004), How important is nucleation in regional/global modelling?, *Geophys. Res. Lett.*, *31*, L12109, doi:10.1029/2004GL019525.

Raes, F. R., V. Dingenen, E. Cuevas, P. F. J. Van Velthoven, and J. M. Prospero (1997), Observations of aerosols in the free troposphere and marine boundary layer of the subtropical northeast Atlantic: Discussion of processes determining their size distributions, *J. Geophys. Res.*, *102*, 21,315–21,328, doi:10.1029/97JD01122.

Sakurai, H., M. A. Fink, P. H. McMurry, L. Mauldin, K. F. Moore, J. N. Smith, and F. L. Eisele (2005), Hygroscopicity and volatility of 4–10 nm particles during summertime atmospheric nucleation events in urban Atlanta, *J. Geophys. Res.*, *110*, D22S04, doi:10.1029/2005JD005918.

Seinfeld, J. H., and S. N. Pandis (2006), *Atmospheric Chemistry and Physics: From Air Pollution to Climate Change*, 2nd ed., 1232 pp., John Wiley, Hoboken, N. J.

Sihto, S., M. Kulmala, V. Kerminen, M. Dal Maso, T. Petäjä, I. Riipinen, H. Korhonen, F. Arnold, R. Janson, and M. Boy (2006), Atmospheric sulphuric acid and aerosol formation: Implications from atmospheric measurements for nucleation and early growth mechanisms, *Atmos. Chem. Phys.*, *6*, 4079–4091, doi:10.5194/acp-6-4079-2006.

Sipilä, M., et al. (2010), The role of sulfuric acid in atmospheric nucleation, *Science*, *327*, 1243–1246, doi:10.1126/science.1180315.

Smith, J. N., K. F. Moore, F. L. Eisele, D. Voisin, A. K. Ghimire, H. Sakurai, and P. H. McMurry (2005), Chemical composition of atmospheric nanoparticles during nucleation events in Atlanta, *J. Geophys. Res.*, *110*, D22S03, doi:10.1029/2005JD005912.

Smith, J. N., K. C. Barsanti, H. R. Friedli, M. Ehn, M. Kulmala, D. R. Collins, J. H. Scheckman, B. J. Williams, and P. H. McMurry (2010), Observations of aminium salt formation in atmospheric nanoparticles and possible climatic implications, *Proc. Natl. Acad. Sci. U. S. A.*, *107*(15), 6634–6639, doi:10.1073/pnas.0912127107.

Spracklen, D. V., et al. (2008), Contribution of particle formation to global cloud condensation nuclei concentrations, *Geophys. Res. Lett.*, *35*, L06808, doi:10.1029/2007GL033038.

Stanier, C. O., A. Y. Khlystov, and S. N. Pandis (2004), Nucleation events during the Pittsburgh air quality study: Description and relation to key meteorological, gas phase, and aerosol parameters, *Aerosol Sci. Technol.*, *38*, 13,253–12,264, doi:10.1080/02786820390229570.

Stolzenburg, M. R., P. H. McMurry, H. Sakurai, J. N. Smith, R. L. Mauldin, F. L. Eisele, and C. F. Clement (2005), Growth rates of freshly nucleated atmospheric particles in Atlanta, *J. Geophys. Res.*, *110*, D22S05, doi:10.1029/2005JD005935.

van Dingenen, R., and F. Raes (1993), Ternary nucleation of methane sulphonic acid, sulphuric acid and water vapour, *J. Aerosol Sci.*, *24*, 1–17, doi:10.1016/0021-8502(93)90081-J.

Van Loy, M., T. Bahadori, R. Wyzga, B. Hartsell, and E. Ederton (2000), The aerosol research and inhalation epidemiology study (ARIES), $PM_{2.5}$ mass and aerosol component concentrations and sampler intercomparisons, *J. Air Waste Manage. Assoc.*, *50*, 1446–1458.

Vehkamäki, H., M. Kulmala, I. Napari, K. E. J. Lehtinen, C. Timmreck, M. Noppel, and A. Laaksonen (2002), An improved parameterization for sulfuric acid-water nucleation rates for tropospheric and stratospheric conditions, *J. Geophys. Res.*, *107*(D22), 4622, doi:10.1029/2002JD002184.

Vehkamäki, H., I. Napari, M. Kulmala, and M. Noppel (2004), Stable ammonium bisulfate clusters in the atmosphere, *Phys. Rev. Lett.*, *93*, 148501, doi:0.113/PhysRevLett.93.14501.

Weber, R. J., J. J. Marti, P. H. McMurry, F. L. Eisele, D. J. Tanner, and A. Jefferson (1997), Measurements of new particle formation and ultrafine particle growth rates at a clean continental site, *J. Geophys. Res.*, *102*, 4375–4385, doi:10.1029/96JD03656.

Weber, R. J., et al. (2003), New particle formation in anthropogenic plumes advecting from Asia observed during TRACE-P, *J. Geophys. Res.*, *108*(D21), 8814, doi:10.1029/2002JD003112.

Wexler, A. S., F. W. Lurmann, and J. H. Seinfeld (1994), Modeling urban and regional aerosols. I. Model development, *Atmos. Environ.*, *28*, 531–546, doi:10.1016/1352-2310(94)90129-5.

Young, L. H., D. R. Benson, F. R. Kameel, and S. H. Lee (2008), Laboratory studies of H_2SO_4/H_2O binary homogeneous nucleation from the SO_2+OH reaction: Evaluation of the experimental setup and preliminary results, *Atmos. Chem. Phys.*, *8*, 4997–5016, doi:10.5194/acp-8-4997-2008.

Yu, F. (2006a), From molecular clusters to nanoparticles: Second-generation ion-mediated nucleation model, *Atmos. Chem. Phys.*, *6*, 5193–5211, doi:10.5194/acp-6-5193-2006.

Yu, F. (2006b), Effect of ammonia on new particle formation: A kinetic H_2SO_4-H_2O-NH_3 nucleation model constrained by laboratory measurements, *J. Geophys. Res.*, *111*, D01204, doi:10.1029/2005JD005968.

Yu, F. (2007), Improved quasi-unary nucleation model for binary H_2SO_4-H_2O homogeneous nucleation, *J. Chem. Phys.*, *127*, 054301, doi:10.1063/1.2752171.

Yu, F. (2008), Updated H_2SO_4-H_2O binary homogeneous nucleation rate look-up tables, *J. Geophys. Res.*, *113*, D24201, doi:10.1029/2008JD010527.

Yu, F. (2010), Ion-mediated nucleation in the atmosphere: Key controlling parameters, implications, and look-up table, *J. Geophys. Res.*, *115*, D03206, doi:10.1029/2009JD012630.

Yu, F., and G. Luo (2009), Simulation of particle size distribution with a global aerosol model: Contribution of nucleation to aerosol and CCN number concentrations, *Atmos. Chem. Phys.*, *9*, 7691–7710, doi:10.5194/acp-9-7691-2009.

Yu, F., and R. P. Turco (2000), Ultrafine aerosol formation via ion-mediated nucleation, *Geophys. Res. Lett.*, *27*(6), 883–886, doi:10.1029/1999GL011151.

Yu, F., and R. P. Turco (2001), From molecular clusters to nanoparticles: Role of ambient ionization in tropospheric aerosol formation, *J. Geophys. Res.*, *106*, 4797–4814, doi:10.1029/2000JD900539.

Yu, F., Z. Wang, G. Luo, and R. P. Turco (2008), Ion-mediated nucleation as an important source of tropospheric aerosols, *Atmos. Chem. Phys.*, *8*, 2537–2554, doi:10.5194/acp-8-2537-2008.

Yu, F., G. Luo, T. S. Bates, B. Anderson, A. Clarke, V. Kapustin, B. Yantosca, Y.-X. Wang, and S.-L. Wu (2010), Spatial distributions of particle number concentrations in the global troposphere: Simulations, observations, and implications for nucleation mechanisms, *J. Geophys. Res.*, *115*, D17205, doi:10.1029/2009JD013473.

Zhang, Q., C. O. Stanier, M. R. Canagaratna, J. T. Jayne, D. R. Worsnop, S. N. Pandis, and J. L. Jimenez (2004), Insights into the chemistry of new particle formation and growth events in Pittsburgh based on aerosol mass spectrometry, *Environ. Sci. Technol.*, *38*(18), 4797–4809, doi:10.1021/es035417u.

Zhang, R., I. Suh, J. Zhao, D. Zhang, E. C. Fortner, X. Tie, L. T. Molina, and M. J. Molina (2004), Enhanced atmospheric new particle formation by organic acids, *Science*, *304*, 1487–1490, doi:10.1126/science.1095139.

Zhang, Y., C. Seigneur, J. H. Seinfeld, M. Z. Jacobson, and F. S. Binkowski (1999), Simulation of aerosol dynamics), A comparative review of algorithms used in air quality models, *Aerosol Sci. Technol.*, *31*, 487–514, doi:10.1080/027868299304039.

Zhang, Y., B. Pun, K. Vijayaraghavan, S.-Y. Wu, C. Seigneur, S. Pandis, M. Jacobson, A. Nenes, and J. Seinfeld (2004), Development and application of the model for aerosol dynamics, reaction, ionization and dissolution (MADRID), *J. Geophys. Res.*, *109*, D01202, doi:10.1029/2003JD003501.

Zhang, Y., Y.-S. Chen, P. Pillai, and X.-Y. Dong (2009), Sensitivity of simulated aerosol and cloud properties to nucleation parameterizations in 3-D regional and global models, paper presented at 28th Annual Meeting, AAAR, Minneapolis, Minn.

Zhang, Y., P. Liu, X.-H. Liu, M. Z. Jacobson, P. H. McMurry, F. Yu, P. V. Bhave, S.-C. Yu, and K. L. Schere (2010), A comparative study of nucleation parameterizations: 2. Three-dimensional model simulations and evaluation, *J. Geophys. Res.*, in press.

M. Z. Jacobson, Department of Civil and Environmental Engineering, Stanford University, Stanford, CA 94305, USA.

P. H. McMurry, Department of Mechanical Engineering, University of Minnesota-Twin Cities, Minneapolis, MN 55455, USA.

F. Yu, Atmospheric Sciences Research Center, State University of New York at Albany, Albany, NY 12222, USA.

Y. Zhang, Department of Marine, Earth, and Atmospheric Sciences, North Carolina State University, Campus Box 8208, Raleigh, NC 27695, USA. (yang_zhang@ncsu.edu)